ACS OMEGA

Article

Cite This: ACS Omega 2018, 3, 2865−2882

Highly Potent, Stable, and Selective Dimeric Hetarylpropylguanidine-Type Histamine H_2 Receptor Agonists†

Steffen Pockes,* David Wifling, Max Keller, Armin Buschauer, and Sigurd Elz

Institute of Pharmacy, Faculty of Chemistry and Pharmacy, University of Regensburg, Universitätsstraße 31, D-93053 Regensburg, Germany

Supporting Information

ABSTRACT: On the basis of the long-known prototypic pharmacophore 3-(1*H*-imidazol-4-yl)propylguanidine (SK&F 91486, **2**), monomeric, homodimeric, and heterodimeric bisalkylguanidine-type histamine H_2 receptor (H_2R) agonists with various alkyl spacers were synthesized. Aiming at increased H_2R selectivity of the ligands, the imidazol-4-yl moiety was replaced by imidazol-1-yl, 2-aminothiazol-5-yl or 2-amino-4-methylthiazol-5-yl according to a bioisosteric approach. All compounds turned out to be partial or full agonists at the $h/gp/rH_2R$. The most potent analogue, the thiazole-type heterodimeric ligand **63** (UR-Po461), was a partial agonist (E_{max} = 88%) and 250 times more potent than histamine (pEC_{50}: 8.56 vs 6.16, gpH_2R, atrium). The homodimeric structures **56** (UR-Po395) and **58** (UR-Po448) exhibited the highest hH_2R affinities (pK_i: 7.47, 7.33) in binding studies. Dimeric amino(methyl)thiazole derivatives, such as **58**, generated an increased hH_2R selectivity compared to the monomeric analogues, e.g., **139** (UR-Po444). Although monomeric ligands showed up lower affinities and potencies at the H_2R, compounds with a short alkylic side chain like **129** (UR-Po194) proved to be highly affine hH_4R ligands.

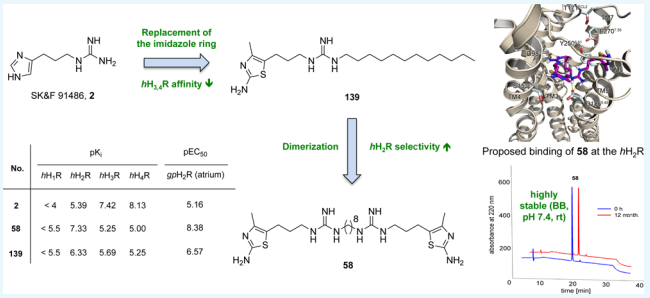

1. INTRODUCTION

In humans, the histamine receptor family comprises four subtypes, namely, H_1, H_2, H_3, and H_4 receptors.[1−4] They are activated by the biogenic amine histamine (**1**, Figure 1)[5] and belong to the superfamily of G-protein-coupled receptors (GPCRs).[6] For more than three decades, 3-(1*H*-imidazol-4-yl)propylguanidine (SK&F 91486, **2**, Figure 1)[7] has been used as prototypic pharmacophore for the synthesis of highly potent histamine H_2-receptor (H_2R) agonists of the guanidine class, e.g., compounds such as arpromidine (**3**, Figure 1).[8] The application of the bivalent ligand approach to acylguanidine-type H_2R agonists by Birnkammer et al. led to highly potent and selective H_2R agonists, e.g., UR-AK 381 (**4**, Figure 1), raising questions about the binding mode and usability of such dimeric ligands as pharmacological tools.[9] Insufficient chemical stability of these acylguanidines, due to hydrolytic cleavage, led to carbamoylguanidine-type H_2R agonists, which proved to be stable.[10] As many class A GPCRs were reported to form homo- and heterodimers, bivalent ligands can potentially be used as pharmacological tools to investigate the binding mode.[11,12] Using different spacer lengths, Birnkammer et al. showed that an interaction of the second pharmacophore with an allosteric binding site at the same receptor protomer is more likely than binding to the second orthosteric binding site of an H_2R homodimer.[9]

For a better understanding of the structure−activity relationship of bisalkylguanidine-type dimeric H_2R ligands, we prepared and pharmacologically characterized several monomeric and dimeric compounds derived from the recently reported homodimeric H_2R agonist SK&F 93082 (**5**, Figure 1).[13] In particular, the influence of different heteroaromatic ring systems and different spacer lengths on histamine receptor subtype selectivity was studied, using radioligand binding assays to investigate the affinities to the respective receptors. Investigations on H_2R species selectivity were performed involving recombinant human, guinea pig, and rat H_2Rs ([^{35}S]GTPγS binding assay),[14] which gave information about the type, affinity/potency, and efficacy of the receptor ligand. Organ pharmacological studies (gpH_1R (ileum), gpH_2R (right atrium))[15,16] afforded agonistic (H_2R) and antagonistic (H_1R) activities under more physiological conditions. Functional activities on the guinea pig ileum and right atrium were measured via the contractility of the tissue and the increase of the heart frequency, respectively. The main focus of this project was the development of H_2R agonists. This also includes the characterization of numerous compounds at the other histamine receptors ($H_{1,3,4}R$), which led to the identification of selective H_4R ligands.

2. RESULTS AND DISCUSSION

2.1. Chemistry. The structures of amines **6**−**9**, which were used for the synthesis of compounds **5**, **53**−**63**, **127**−**141**, and

Received: January 22, 2018
Accepted: February 13, 2018
Published: March 9, 2018

DOI: 10.1021/acsomega.8b00128
ACS Omega 2018, 3, 2865−2882

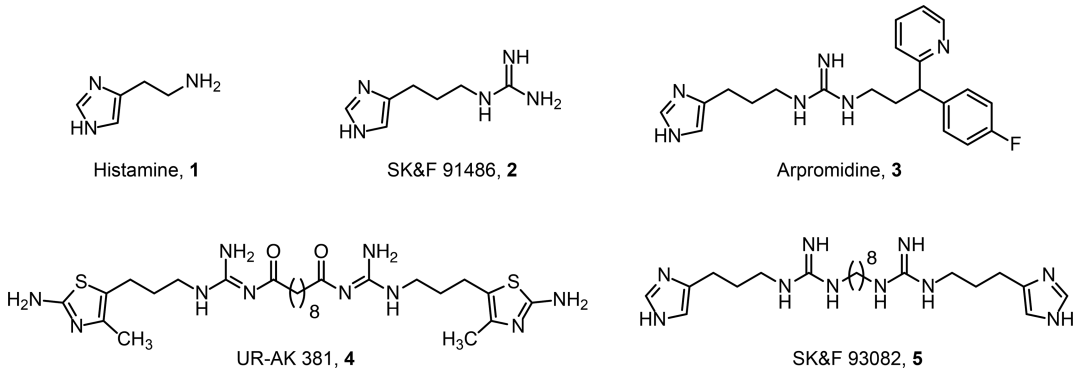

Figure 1. Structures of histamine and selected H_2R agonists (**2**–**5**).

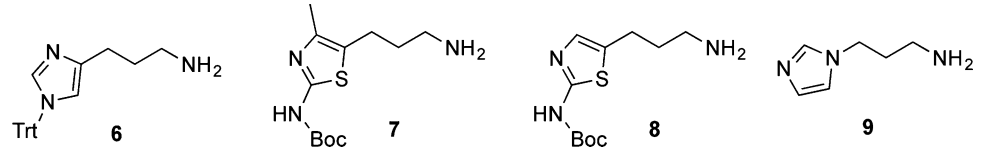

Figure 2. Structures of the building blocks **6**–**9**, which were used for the preparation of the dimeric and monomeric compounds **5**, **53**–**63**, **127**–**141**, and **145** (cf. scheme 1–3).

145, are depicted in Figure 2. For the preparation of the dimeric ligands, the diamines **11**–**16** were treated with benzoyl isothiocyanate (**10**) to give the corresponding dibenzoylthioureas **17**–**22** (Scheme 1) via nucleophilic addition, followed by alkaline hydrolysis yielding the bisthioureas **23**–**28** as described.[17,8] After *S*-methylation using methyl iodide, the bis(*S*-methylisothioureas) **29**–**34** were Boc-protected to give the guanidinylation reagents **35**–**40** (Scheme 1) following reported procedures.[8,18] The homodimeric ligands **5**, **53**–**60** were obtained by treating amines **6**, **7**, **8**, or **9** (each 2 equiv) with some of the guanidinylation reagents **35**–**40** in the presence of $HgCl_2$ (2 equiv) and triethylamine (NEt_3),[19] followed by Boc deprotection of the intermediates **41**–**49**. The heterodimeric ligands **61**–**63** were synthesized by treatment of the guanidinylating reagent **38** with an equimolar mixture of two different amines (**6** and **7**, **6** and **8**, or **7** and **8**), followed by deprotection of the intermediates **50**–**52** using trifluoroacetic acid (TFA, Scheme 1). It should be mentioned that the use of more than 2 equiv of $HgCl_2$ led to a decrease in yield, presumably due to conversion of one *S*-methylisothiourea moiety to the respective carbodiimide as described in the literature.[18,19]

The synthetic strategy for the dimeric compounds was also used for the synthesis of the monomeric compounds **127**–**141** (Scheme 2). Although the alkylated thioureas **82**–**87** were commercially available, **76**–**81** had to be synthesized by nucleophilic addition of the corresponding amine (**64**–**69**) with **10** to give **70**–**75**, followed by alkaline hydrolysis yielding the desired compounds (cf. Scheme 2). S-methylation (**88**–**99**), Boc-protection (**100**–**111**), and guanidinylation (**112**–**126**) were accomplished as described for the dimeric ligands with adapted amount of substance (Scheme 2). Finally, the precursors **112**–**126** were deprotected using TFA to give **127**–**141** (Scheme 2).

The cyclic guanidine derivative *N*-[3-(1*H*-imidazol-4-yl)-propyl]-1,4,5,6-tetrahydropyrimidin-2-amine (**145**) was prepared in a three-step synthesis starting from tetrahydropyrimidine-2(1*H*)-thione (**142**) (Scheme 3). Di-Boc-protection of **142** in the presence of sodium hydride resulted in **143** (Scheme 3), as described.[20] After guanidinylation with **6**, intermediate **144** was treated with TFA to receive **145** (Scheme 3).

2.2. Stability of Dimeric Alkylguanidines. The chemical stability of the bisalkylguanidine-type dimeric HR ligands was exemplarily investigated for compounds **57** and **58**, which were incubated in a binding buffer (BB, pH 7.4) at a concentration of 100 μM at room temperature for 12 months. Reversed-phase high-performance liquid chromatography (RP-HPLC) analysis revealed that **57** and **58** exhibited, in contrast to the previously reported acylguanidine-type HR ligands,[10] excellent chemical stabilities (Figure 3).

2.3. Pharmacology. The synthesized dimeric (**5**, **53**–**63**) and monomeric (**127**–**141** and **145**) ligands were investigated in radioligand competition binding assays ($hH_{1,2,3,4}R$), in the [^{35}S]GTPγS binding assay ($hH_{2,3,4}R$, gp/rH_2R), in the guinea pig ileum assay (gpH_1R), and in the guinea pig right atrium assay (gpH_2R). For the radioligand and the GTPγS binding assay, membranes of Sf9 cells, expressing hH_1R + RGS4, $h/gp/rH_2R$ + $G_s\alpha_s$, hH_3R + $G_i\alpha_2$ + $G\beta_1\gamma_2$, or hH_4R $G_i\alpha_2$ + $G\beta_1\gamma_2$, were used.

2.3.1. Receptor Subtype Selectivity. To investigate the affinities of **5**, **53**–**63**, **127**–**141**, and **145** at the four *h*HR subtypes, competition binding studies were performed using the radioligands [^{3}H]mepyramine (hH_1R), [^{3}H]tiotidine or [^{3}H]UR-DE257[21] (hH_2R), [^{3}H]N^{α}-methylhistamine (hH_3R), and [^{3}H]histamine (hH_4R). The imidazol-4-yl-type homodimeric ligands **56** and **57**, containing a decamethylene and a dodecamethylene spacer, respectively, exhibited the highest affinities at every HR subtype with the following selectivity profile: pK_i $H_1R < H_2R \approx H_3R \approx H_4R$ (Table 1). The same selectivity profile was evident for the homodimeric compounds **5** and **53**–**55**. The 2-amino-4-methylthiazol-5-yl- and 2-aminothiazol-5-yl-type homodimeric ligands **58** and **59**, respectively, as well as the 2-amino-4-methylthiazol-5-yl/2-aminothiazol-5-yl-type heterodimeric compound **63** proved to be selective H_2R ligands with at least 1.5 log units difference in pK_i (H_2R) over pK_i ($H_{1,3,4}R$) (Table 1). This demonstrated that replacement of the imidazol-4-yl by an 2-aminothiazol-5-yl moiety is bioisosteric with respect to H_2R binding, but not in

DOI: 10.1021/acsomega.8b00128
ACS Omega 2018, 3, 2865–2882

Scheme 1. Synthesis of the Homodimeric (5, 53−60) and Heterodimeric (61−63) Histamine Receptor (HR) Ligands[a]

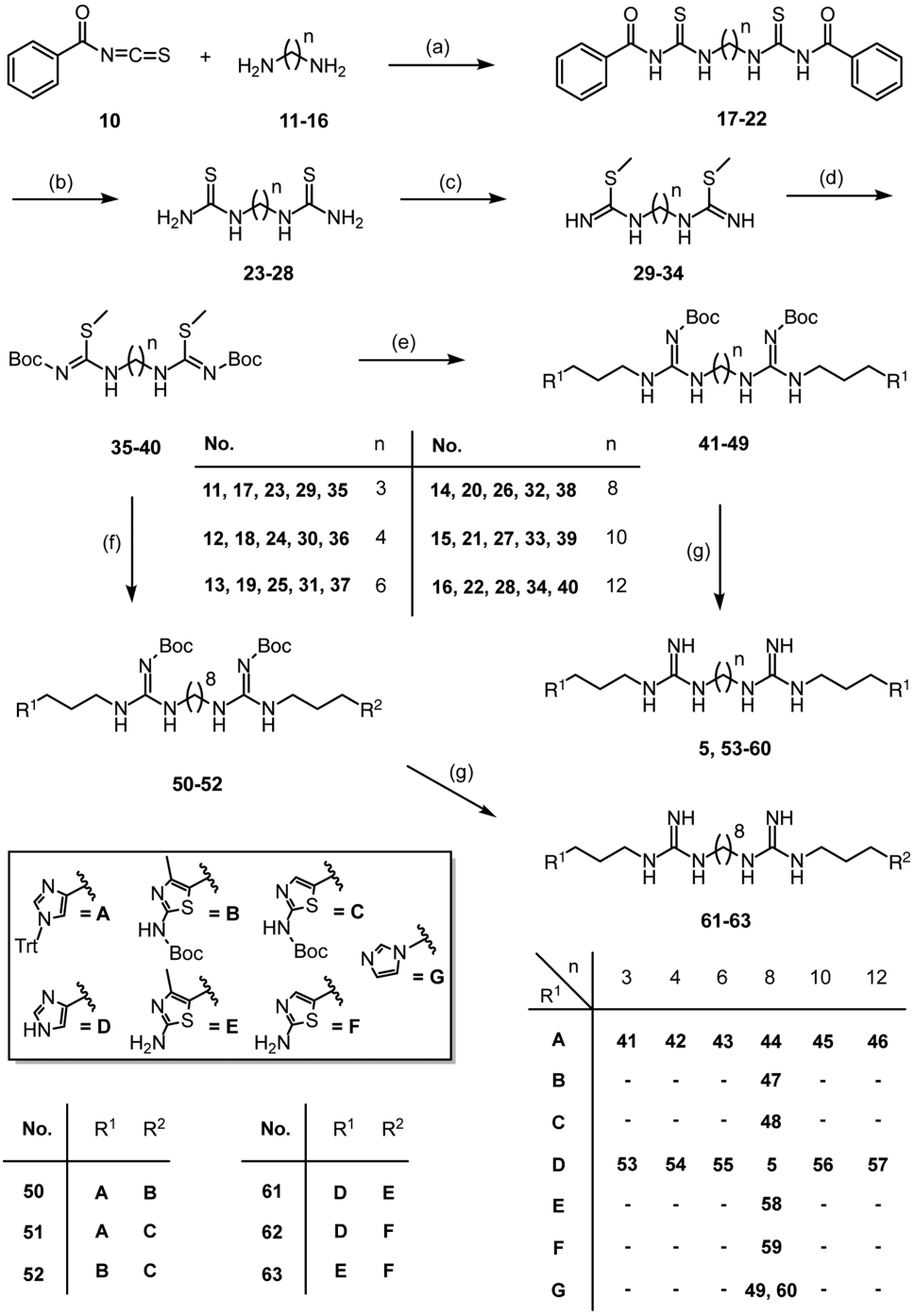

No.	n	No.	n
11, 17, 23, 29, 35	3	14, 20, 26, 32, 38	8
12, 18, 24, 30, 36	4	15, 21, 27, 33, 39	10
13, 19, 25, 31, 37	6	16, 22, 28, 34, 40	12

No.	R^1	R^2	No.	R^1	R^2
50	A	B	61	D	E
51	A	C	62	D	F
52	B	C	63	E	F

R^1 \ n	3	4	6	8	10	12
A	41	42	43	44	45	46
B	-	-	-	47	-	-
C	-	-	-	48	-	-
D	53	54	55	5	56	57
E	-	-	-	58	-	-
F	-	-	-	59	-	-
G	-	-	-	49, 60	-	-

[a]Reagents and conditions: (a) diamine (1 equiv), **10** (2 equiv), dichloromethane (DCM), overnight, 0 °C → room temperature (rt); (b) K_2CO_3 (4.1 equiv), MeOH/H_2O (7/3, v/v), 3−5 h, rt; (c) CH_3I (2.1 equiv), MeCN, 1 h, reflux; (d) NEt_3 (2 equiv), di-*tert*-butyl dicarbonate (Boc_2O) (2 equiv), overnight, rt; (e) **6**, **7**, **8**, or **9** (2 equiv), $HgCl_2$ (2 equiv), NEt_3 (6 equiv), DCM, overnight, rt; (f) equimolar mixtures (each 1 equiv) of **6** and **7**, **6** and **8**, or **7** and **8**, $HgCl_2$ (2 equiv), NEt_3 (6 equiv), DCM, overnight, rt; (g) 20% TFA, DCM, overnight, reflux.

case of H_3 and H_4 receptor binding, and was in accordance with previous reports on 2-aminothiazol-5-yl-type H_2R selective ligands.[22] The binding data at the hH_1R showed values, which were dependent from the spacer length, respectively the lipophilicity. The replacement of imidazol-4-yl by a imidazol-1-yl ring (**60**) leads to a collapse of the affinities at all histamine receptor subtypes. The monomeric reference substances **127**−**141** and **145** displayed increasing affinities at the hH_2R with respect to their chain length, but lower affinities compared to the respective dimeric compounds. Overall, the affinities at the $hH_{3,4}Rs$ were higher, except of the aminothiazole-containing structures **139**−**140**. Molecules with a small side chain like **129** are of special interest as highly affine hH_4R ligands. Sigmoidal radioligand displacement curves at all HR subtypes are shown for **58**, which exhibited the highest H_2R selectivity (Figure 4).

2.3.2. Functional Characterization at the $hH_{2,3,4}R$ ([^{35}S]GTPγS Binding Assay). The compounds **5**, **57**−**59**, **61**−**63**, **136**, and **139** were chosen to be investigated in the

DOI: 10.1021/acsomega.8b00128
ACS Omega 2018, 3, 2865−2882

Scheme 2. Synthesis of the Monomeric HR Ligands 127−141[a]

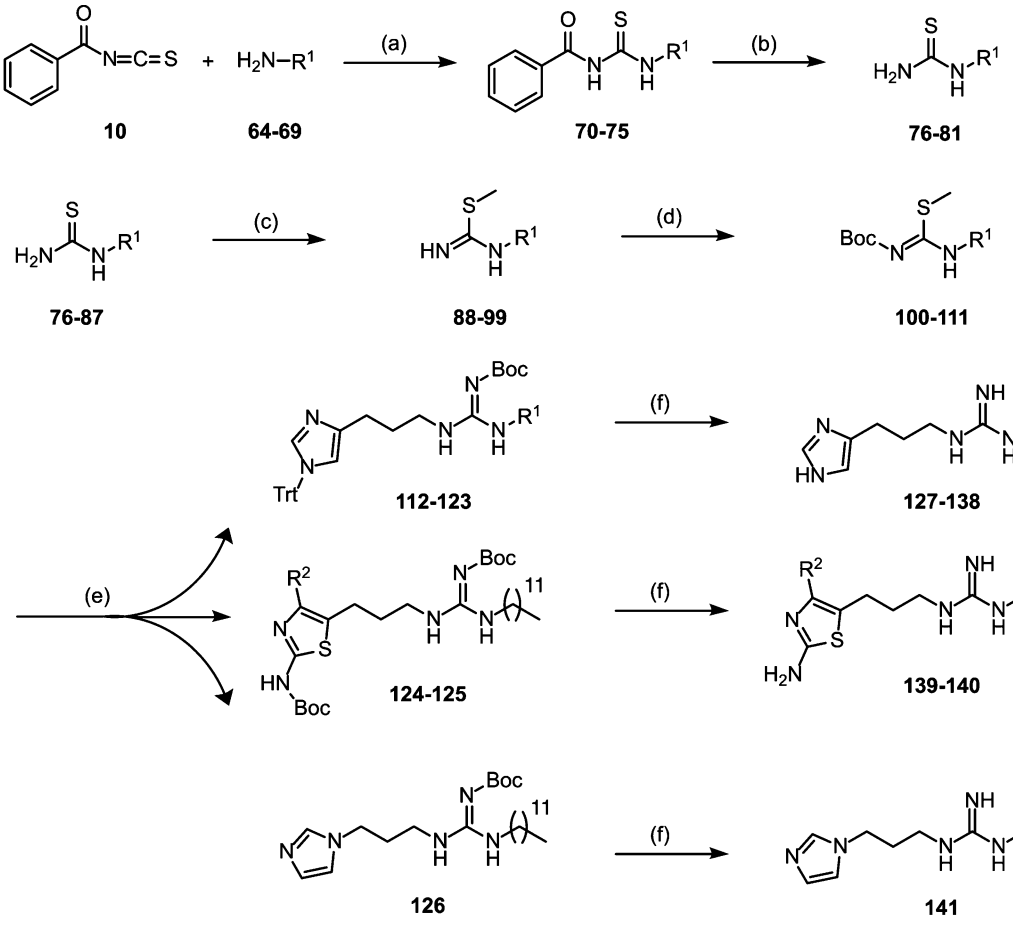

No.	R^1	No.	R^1
82, 88, 100, 112, 127	CH_3	87, 94, 106, 118, 133	$C(CH_3)_3$
83, 89, 101, 113, 128	CH_2-CH_3	65, 71, 77, 95, 107, 119, 134	$(CH_2)_4$-CH_3
84, 90, 102, 114, 129	$(CH_2)_2$-CH_3	66, 72, 78, 96, 108, 120, 135	$(CH_2)_2$-CH-$(CH_3)_2$
85, 91, 103, 115, 130	$CH(CH_3)_2$	67, 73, 79, 97, 109, 121, 136	$(CH_2)_7$-CH_3
86, 92, 104, 116, 131	$(CH_2)_3$-CH_3	68, 74, 80, 98, 110, 122, 137	$(CH_2)_9$-CH_3
64, 70, 76, 93, 105, 117, 132	CH_2-CH-$(CH_3)_2$	69, 75, 81, 99, 111, 123, 138	$(CH_2)_{11}$-CH_3

R^2		
CH_3	124	139
H	125	140

[a]Reagents and conditions: (a) amine (1 equiv), **10** (1 equiv), MeCN, 2 h, 0 °C → rt; (b) K_2CO_3 (2.1 equiv), MeOH/H_2O (7/3, v/v), 3−5 h, rt; (c) CH_3I (1.1 equiv), MeCN, 1 h, reflux; (d) NEt_3 (1 equiv), Boc_2O (1 equiv), overnight, rt; (e) **6**, **7**, **8**, or **9** (1 equiv), $HgCl_2$ (2 equiv), NEt_3 (3 equiv), DCM, overnight, rt; (f) 20% TFA, DCM, overnight, reflux.

[^{35}S]GTPγS binding assay to determine their agonistic or antagonistic activities at the hH$_{2,3,4}$R (Table 2). All compounds proved to be partial agonists at the hH$_2$R and silent antagonists at the hH$_3$R and hH$_4$R, except the monomeric ligands **136** and **139**, which exhibited inverse agonistic activity at the hH$_3$R and the hH$_4$R, respectively. The homodimeric ligand **58**, containing a C_{12}-spacer, showed the highest H_2R potency with a pEC_{50} of 7.27 and a maximal response of 52% relative to histamine. At the H_3R, the antagonistic activities of imidazole-containing ligands (**5**, **57**, **61**, **62**, and **136**) were considerably higher than those of compounds with an amino(methyl)thiazole moiety (**58**, **59**, **63**, and **139**) (e.g., pK_B values of **57** and **59**: 7.33 vs 4.05; Table 2). Antagonistic activities at the hH$_4$R were throughout low (pK_B < 4).

2.3.3. H_2R Species Selectivity. To study the H_2R species selectivity of the bisalkylguanidine-type dimeric ligands, the agonistic activities of compounds **5**, **57**, **58**, and **63** were also investigated at the gpH$_2$R and rH$_2$R in the GTPγS binding assay. The studied compounds exhibited slightly higher agonistic potencies at the gpH$_2$R and rH$_2$R compared to the

DOI: 10.1021/acsomega.8b00128
ACS Omega 2018, 3, 2865−2882

Scheme 3. Synthesis of *N*-[3-(1*H*-Imidazol-4-yl)propyl]-1,4,5,6-tetrahydropyrimidin-2-amine (145)[a]

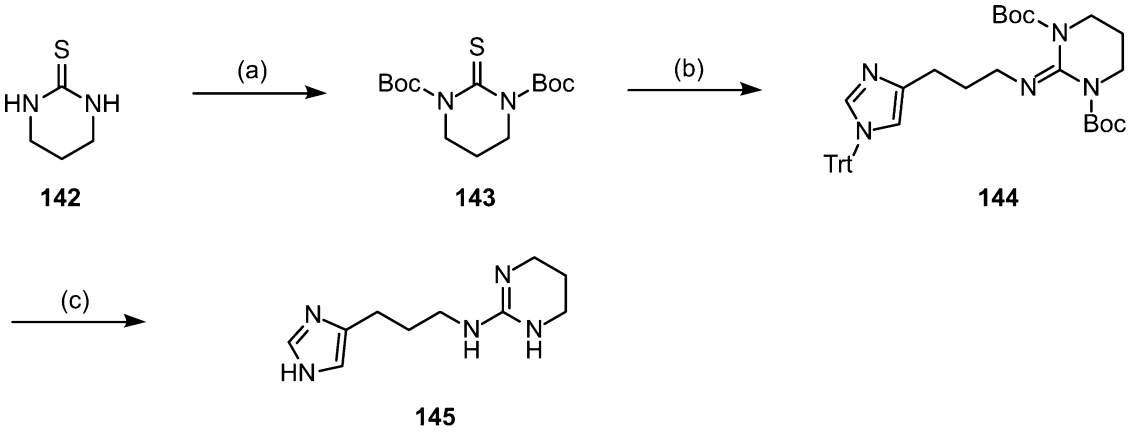

[a]Reagents and conditions: (a) tetrahydropyrimidine-2(1*H*)-thione (1 equiv), NaH (4.5 equiv), Boc_2O (2.2 equiv), tetrahydrofuran (THF), hexane, 2 h, 0 °C → rt; (b) **6** (1 equiv), $HgCl_2$ (2 equiv), NEt_3 (3 equiv), DCM, overnight, rt; (c) 20% TFA, DCM, overnight, reflux.

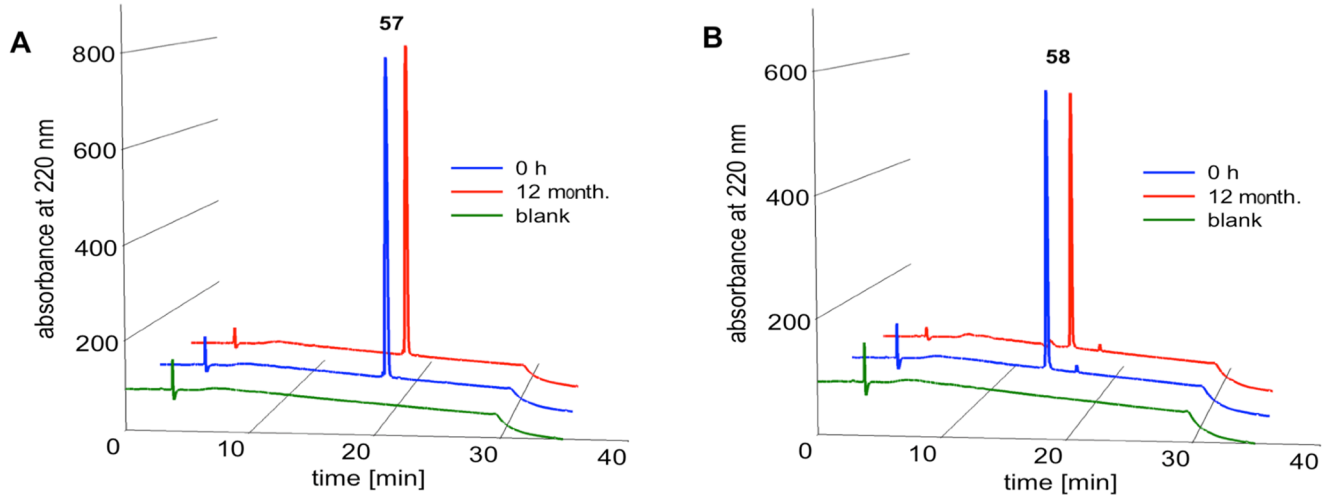

Figure 3. RP-HPLC images of **57** (A) and **58** (B) after incubation in BB (pH 7.4) at rt for 12 months. Both compounds showed no decomposition.

hH_2R, with pEC_{50} values >7.2 and >6.8, respectively (Table 3). Compound **5** showed the highest gpH_2R potency (pEC_{50} = 7.60) with a high efficacy (E_{max} = 0.95), and **57** displayed the highest rH_2R potency (pEC_{50} = 7.61) with an efficacy of 0.80. In general, the efficacies were considerably higher at the gpH_2R and rH_2R (E_{max} > 0.7) compared to the hH_2R (E_{max} < 0.52), reaching full agonism in case of compound **63** (gpH_2R, E_{max} = 1.02). In sum, these investigations revealed that the highest potencies and efficacies were observed at the gpH_2R followed by the rH_2R and the hH_2R.

2.3.4. Organ Bath Studies. In addition to the pharmacological characterization by radioligand competition binding (cf. Table 1) and by functional studies using the [^{35}S]GTPγS binding assay (cf. Tables 2 and 3), organ bath experiments at the guinea pig ileum (gpH_1R) and at the spontaneously beating guinea pig right atrium (gpH_2R) were carried out. All ligands (**5**, **53**−**63**, **127**−**141**, and **145**) displayed antagonistic activities at the gpH_1R (Table 4). The imidazol-4-yl-type homodimeric ligands **57** and the monomeric compound **137**, containing a dodecamethylene spacer and a decamethyl side chain, respectively, showed the highest pA_2 values (6.91 and 6.74, respectively, cf. Table 4). A variation of the heteroaromatic moieties did almost not affect the pA_2 value (gpH_1R), as shown for compounds containing a C_8-spacer (**5** and **58**−**63**). The experiments at the gpH_2R provided interesting information about the structure−activity relationship from monomeric and dimeric HR ligands. Regarding the imidazole-containing ligands (**5**, **53**−**57**, and **127**−**138**), longer alkyl spacers resulted in higher agonistic potencies (e.g., pEC_{50} of **53** (C_3-spacer) and **57** (C_{12}-spacer): 7.31 vs 8.11, pEC_{50} of **127** (methyl) and **138** (dodecyl): 5.10 vs 6.63). By contrast, an inverse correlation was observed for the dimeric compounds with respect to the efficacy: compound **53**, containing a C_3-spacer, acted nearly as a full agonist (E_{max} = 0.96), and **57**, containing a C_{12}-chain, exhibited a maximum response of 0.63 compared to histamine (Table 4). With the aim of getting compounds of highest potency and efficacy, **58**−**63** were equipped with a C_8-spacer with **5** (pEC_{50} = 7.98, E_{max} = 0.91) as a prototype. The replacement of imidazol-4-yl (**5** and **138**) by imidazol-1-yl (**60** and **141**) led to a drastic decrease in potency and efficacy (**5** vs **60**: pEC_{50}: 7.98 vs 5.31, E_{max}: 0.91 vs 0.20; **138** vs **141**: pEC_{50}: 6.63 vs not active, E_{max}: 0.91 vs 0). The introduction of amino(methyl)thiazole moieties (**58**, **59**, and **61**−**63**) resulted in potent gpH_2R agonists (pEC_{50}: 7.69−8.56, E_{max}: 0.78−1.02, Table 4). Overall, a switch from monomeric to dimeric ligands revealed compounds, which are approximately 100 times more potent than their monomeric analogues. The concentration−

DOI: 10.1021/acsomega.8b00128
ACS Omega 2018, 3, 2865−2882

Table 1. Binding Data (pK_i Values) of Compounds Diphenhydramine (DPH), 1, 2, 5, 53−63, 127−141, and 145 Determined at Human H_xRs (x = 1−4)[a]

	hH_1R[b]		hH_2R[c]		hH_3R[d]		hH_4R[e]	
compound	pK_i	N	pK_i	N	pK_i	N	pK_i	N
DPH	7.62 ± 0.01	4	n.d.[g]		n.d.		n.d.	
1	5.62 ± 0.03[23]	3	6.58 ± 0.04	48	7.59 ± 0.01	42	7.60 ± 0.01	45
2	<4	3	5.39 ± 0.04[f]	3	7.42 ± 0.04	3	8.13 ± 0.08	3
5	5.50 ± 0.01	2	7.05 ± 0.02	3	7.52 ± 0.01	3	7.06 ± 0.01	3
53	<5	2	6.76 ± 0.03	3	6.95 ± 0.02	3	6.70 ± 0.01	3
54	<5	2	6.39 ± 0.02	3	6.84 ± 0.01	3	6.18 ± 0.04	3
55	<5.5	2	6.82 ± 0.04	3	7.28 ± 0.03	3	6.37 ± 0.02	3
56	5.90 ± 0.01	2	7.47 ± 0.12	3	7.72 ± 0.03	3	7.68 ± 0.04	3
57	6.45 ± 0.01	2	7.41 ± 0.03	3	7.79 ± 0.01	3	7.70 ± 0.01	3
58	<5.5	2	7.33 ± 0.05	3	5.25 ± 0.05	3	5.00 ± 0.05	3
59	<5	2	6.63 ± 0.03	3	4.96 ± 0.05	3	4.28 ± 0.02	3
60	<5	2	5.35 ± 0.03	3	5.56 ± 0.02	3	4.47 ± 0.03	3
61	<6	2	6.93 ± 0.04	3	7.49 ± 0.03	3	7.13 ± 0.04	3
62	<6	2	7.27 ± 0.04	3	7.43 ± 0.03	3	6.97 ± 0.05	3
63	<5.5	2	6.91 ± 0.04	3	5.40 ± 0.05	3	5.14 ± 0.04	3
127	<4.5	2	5.56 ± 0.07	3	6.81 ± 0.03	3	7.58 ± 0.07	3
128	<4.5	2	5.31 ± 0.05	3	7.03 ± 0.04	3	7.87 ± 0.01	3
129	<4.5	2	5.52 ± 0.05	3	7.21 ± 0.02	3	8.04 ± 0.05	3
130	<5	2	5.38 ± 0.07	3	7.04 ± 0.02	3	7.42 ± 0.01	3
131	<5	2	6.11 ± 0.06	3	7.21 ± 0.04	3	8.04 ± 0.02	3
132	<4.5	2	6.12 ± 0.05	3	7.18 ± 0.03	3	7.75 ± 0.03	3
133	<4	2	5.60 ± 0.10	3	6.43 ± 0.03	3	6.66 ± 0.06	3
134	<5	2	6.03 ± 0.06	3	7.04 ± 0.02	3	8.17 ± 0.04	3
135	<5	2	6.10 ± 0.06	3	6.94 ± 0.04	3	7.60 ± 0.01	3
136	<5.5	2	6.96 ± 0.07	3	6.97 ± 0.04	3	6.90 ± 0.01	3
137	5.70 ± 0.01	2	6.85 ± 0.09	3	7.50 ± 0.03	3	7.01 ± 0.03	3
138	5.53 ± 0.01	2	6.22 ± 0.01	3	7.53 ± 0.02	3	7.90 ± 0.03	3
139	<5.5	2	6.33 ± 0.04	2	5.69 ± 0.01	3	5.25 ± 0.03	3
140	<5.5	2	6.57 ± 0.03	2	4.85 ± 0.06	3	4.95 ± 0.05	3
141	<5.5	2	5.90 ± 0.01	2	5.19 ± 0.01	3	4.89 ± 0.06	3
145	<5	2	5.50 ± 0.02	2	6.73 ± 0.05	3	7.42 ± 0.01	3

[a]Data represent mean values ± standard error of the mean (SEM) from at least two independent experiments (N), each performed in triplicate. [b]Radioligand competition binding experiments performed with [^{3}H]mepyramine (hH_1R, K_d 4.5 nM, c = 5 nM) at membranes of Sf9 cells expressing the hH_1R + RGS4. [c]Radioligand competition binding experiments performed with [^{3}H]tiotidine (hH_2R, K_d 19.7 nM, c = 10 nM) at membranes of Sf9 cells expressing the hH_2R + $G_s\alpha_s$. [d]Radioligand competition binding experiments performed with [^{3}H]N^α-methylhistamine (hH_3R, K_d 8.6 nM, c = 3 nM) at membranes of Sf9 cells expressing the hH_3R + $G\alpha_{i2}$ + $G\beta_1\gamma_2$. [e]Radioligand competition binding experiments performed with [^{3}H]histamine (hH_4R, K_d 16.0 nM, c = 15 nM) at membranes of Sf9 cells expressing the hH_4R + $G\alpha_{i2}$ + $G\beta_1\gamma_2$. [f]Displacement of [^{3}H]UR-DE257 (hH_2R, K_d 31.3 nM, c = 20 nM) instead of [^{3}H]tiotidine. [g]n.d. = not determined.

response curve (CRC) of **63** (atrium, gpH_2R) is exemplarily shown in Figure 5A.

The maximum response of all H_2R agonists at the right atrium could be completely antagonized by the addition of the H_2R antagonist cimetidine (pA_2 = 6.10[25,26]) (30 μM) after cumulative organ stimulation (**63**, cf. Figure 5A). Full CRCs in the presence of cimetidine (30 μM, 30 min preincubation) were obtained for compounds **5**, **57**, **62**, **63** (Figure 5B), **127**, **128**, **132**, **135**, and **137**. The presence of cimetidine led to a rightward shift of the CRCs in a way that is in accordance with the calculated values via Schild equation (Table S1, Supporting Information). These results proved that the positive chronotropic effect of the investigated (partial) agonists in the guinea pig right atrium assay was mediated via the H_2R.

2.4. Computational Studies. To determine accurate binding modes of the most interesting bivalent compounds **5** and **58** at the hH_2R, and of the monovalent ligand **129** at both the hH_3R and hH_4R, molecular docking studies were performed, coupled with molecular dynamics (MD) simulations and free-energy (molecular mechanics generalized born surface area (MM-GBSA)) calculations. Overall, five promising binding poses for **5** and **58** at the hH_2R, two poses for **129** at the hH_3R, and three poses for **129** at the hH_4R were determined by docking studies. Visual analysis of ligand−receptor complexes refined by molecular dynamics simulations (30 ns) has shown that some poses primarily formed contacts within the orthosteric binding site, whereas other poses additionally interacted with residues of the allosteric site between extracellular loop (ECL)2 and ECL3 (Figures S29−S31 and Table S3). The binding free energies (MM-GBSA) of the respective refined lowest free-energy docking poses (pose 1) of **5** (hH_2R), **58** (hH_2R), **129** (hH_3R), and **129** (hH_4R) amounted to −49.0, −61.5, −30.4, and −46.0 kcal/mol (Figures 6, 7, and S28). Interestingly, compared to the other poses, these lowest free-energy conformations were among those with the strongest H-bond contacts between ligand atoms and acidic amino acids of the orthosteric binding site ($D98^{3.32}$, $D186^{5.42}$ for **5** and **58** at hH_2R, $D114^{3.32}$ for **129** at hH_3R, and

DOI: 10.1021/acsomega.8b00128
ACS Omega 2018, 3, 2865−2882

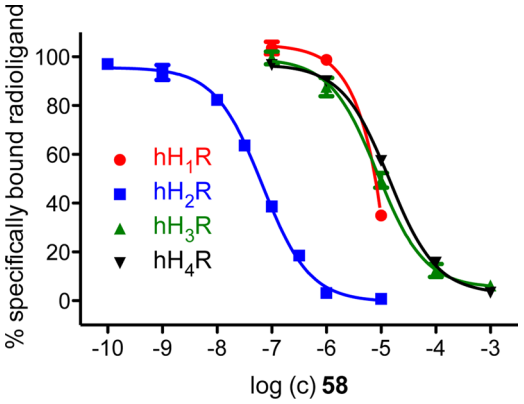

Figure 4. Radioligand displacement curves from radioligand competition binding experiments performed with compound **58** and [^{3}H]mepyramine (hH$_1$R, K_d 4.5 nM, c = 5 nM), [^{3}H]tiotidine (hH$_2$R, K_d 19.7 nM, c = 10 nM), [^{3}H]N^α-methylhistamine (hH$_3$R, K_d 8.6 nM, c = 3 nM), or [^{3}H]histamine (hH$_4$R, K_d 16.0 nM, c = 15 nM) at membranes of Sf9 cells expressing the respective hHR. Data represent mean values ± SEM from at least two independent experiments, each performed in triplicate.

D94$^{3.32}$, E182$^{5.46}$ for **129** at hH$_4$R) (cf. Figure S32). The probability for an interaction with these residues is supported by the fact that they were proven to act as key player in aminergic GPCR activation and ligand binding,[27−30] or to account for receptor selectivity (D186$^{5.42}$ at hH$_2$R).[31] Interestingly, both **5** and **58** showed high binding affinities at hH$_2$R (K_i < 100 nM), low affinities at the hH$_1$R (K_i > 1 μM), but varying affinities at the hH$_3$R and hH$_4$R (**5**: K_i < 100 nM; **58**: K_i > 1 μM). Although, by contrast, the monomeric imidazole-type analogue **129** bound unexpectedly poor to the hH$_2$R, and, comparable to the dimeric compounds, also to the hH$_1$R (K_i > 1 μM), it bound to the hH$_3$R and hH$_4$R with high affinity (K_i < 100 nM). In this context, an amino(methyl)-thiazole moiety present in **58**, unlike an imidazole moiety present in **5** or **129**, was shown to trigger hH$_2$R selectivity also in the case of other ligands.[32,33] Aiming at an attempt to explain this behavior, different steric effects of amino acids enclosing the orthosteric binding pocket may come into play due to less voluminous residues at the hH$_2$R (V99$^{3.33}$, V176$^{ECL2.54}$-Q177$^{ECL2.55}$) compared to hH$_1$R (Y108$^{3.33}$, F184$^{ECL2.54}$-Y185$^{ECL2.55}$), hH$_3$R (Y115$^{3.33}$, F192$^{ECL2.54}$-F193$^{ECL2.55}$), and hH$_4$R (Y95$^{3.33}$, F168$^{ECL2.54}$-F169$^{ECL2.55}$). In addition, an absence (hH$_1$R) or different locations (hH$_3$R: E206$^{5.46}$; hH$_4$R: E182$^{5.46}$) of fundamental acidic amino acids in TM5 compared to hH$_2$R (D186$^{5.42}$) may further contribute to hH$_2$R selectivity of amino(methyl)thiazole-type compounds, but to preferential binding of imidazole-type ligands, such as **5** or **129**, to the hH$_3$R and hH$_4$R. Although **5** is still capable of binding to hH$_2$R, most probably due to its larger and more flexible chain, **129** merely binds to the hH$_3$R and hH$_4$R with high affinity in a well-defined binding mode. Noteworthy, the lowest free-energy pose (pose 1) of **129** bound to the hH$_4$R showed H-bond contacts with E163^{ECL2} and T178$^{5.42}$ in addition to contacts with D94$^{3.32}$ and E182$^{5.46}$, compared to relatively few and weak H-bond interactions when bound to hH$_3$R (Figures 7 and S32). This may contribute to a lower **129** binding free energy when bound to the hH$_4$R, compared to hH$_3$R (Figure S28).

3. SUMMARY AND CONCLUSIONS

Homo- (**5** and **53**−**60**) and heterodimeric (**61**−**63**) as well as monomeric (**127**−**141** and **145**) hetarylpropylguanidine-type HR ligands were obtained in excellent yield by a six-step synthesis. The replacement of the imidazolyl by an amino-thiazolyl moiety led, in accordance with previous reports on acylguanidine- and carbamoylguanidine-type HR ligands,[9,10,22] to highly selective and potent H$_2$R agonists. The variation of the spacer length revealed best results for compounds containing a C$_8$-, C$_{10}$-, or C$_{12}$-spacer (**5**, **56**−**59**, and **61**−**63**). The heterodimeric compounds showed potencies in a one-digit nanomolar range (up to 250 times the potency of histamine) as full agonists in the gpH$_2$R atrium assay. In comparison to the monomeric ligands, the dualsteric structures showed up notably higher hH$_2$R selectivity, higher affinities in the hH$_2$R binding assay, and higher potencies at the functional H$_2$R assays (e.g., guinea pig right atrium). The dimeric ligands displayed a slightly higher sensitivity for gpH$_2$R and rH$_2$R compared to the

Table 2. Agonistic (pEC$_{50}$) and Antagonistic (pK_B) Activities of 1, 2, 5, 57−59, 61−63, 136, and 139 at the hH$_{2,3,4}$R Determined in the [^{35}S]GTPγS Binding Assay[a]

	hH$_2$R[b]			hH$_3$R[c]			hH$_4$R[d]		
compound	pEC$_{50}$[e]	E_{max}[f]	N	pEC$_{50}$[e] (pK_B)[g]	E_{max}[f]	N	pEC$_{50}$[e] (pK_B)[g]	E_{max}[f]	N
1	6.01 ± 0.07	1.00	7	8.52 ± 0.10	1.00	6	8.20 ± 0.08	1.00	3
2	5.59 ± 0.01[h,24]	0.66 ± 0.02[h,24]	3	8.12 ± 0.10[h,24]	0.69 ± 0.04[h,24]	3	8.09 ± 0.04[h,24]	0.83 ± 0.01[h,24]	3
5	6.78 ± 0.01	0.50 ± 0.03	6	(6.87 ± 0.05)	0	3	(3.39 ± 0.02)	0	3
57	7.27 ± 0.05	0.52 ± 0.03	6	(7.33 ± 0.07)	0	3	(3.49 ± 0.01)	0	3
58	6.61 ± 0.03	0.33 ± 0.03	5	(4.53 ± 0.05)	0	3	(3.83 ± 0.03)	0	3
59	6.53 ± 0.08	0.40 ± 0.05	3	(4.05 ± 0.10)	0	3	(3.58 ± 0.05)	0	3
61	6.23 ± 0.09	0.54 ± 0.05	3	(7.18 ± 0.02)	0	3	(3.69 ± 0.02)	0	3
62	6.51 ± 0.03	0.45 ± 0.04	3	(7.09 ± 0.01)	0	3	(3.43 ± 0.01)	0	3
63	6.60 ± 0.02	0.47 ± 0.03	6	(4.67 ± 0.05)	0	3	(3.73 ± 0.03)	0	3
136	6.86 ± 0.08	0.48 ± 0.02	3	7.54 ± 0.06	−0.53 ± 0.03	3	(3.68 ± 0.01)	0	3
139	5.16 ± 0.03	−0.43 ± 0.01	3	(5.37 ± 0.04)	0	3	4.86 ± 0.03	−0.97 ± 0.01	3

[a]Data represent mean values ± SEM from at least three independent experiments (N), each performed in triplicate. Data were analyzed by nonlinear regression and were best-fitted to sigmoidal concentration−response curves (CRCs). [b][^{35}S]GTPγS binding assay at membranes of Sf9 cells expressing the hH$_2$R + G$_s\alpha_s$. [c][^{35}S]GTPγS binding assay at membranes of Sf9 cells expressing the hH$_3$R + Gα_{i2} + G$\beta_1\gamma_2$. [d][^{35}S]GTPγS binding assay at membranes of Sf9 cells expressing the hH$_4$R + Gα_{i2} + G$\beta_1\gamma_2$. [e]pEC$_{50}$: −log EC$_{50}$. [f]E_{max}: maximal response relative to histamine (E_{max} = 1.00). [g]For determination of antagonism, reaction mixtures contained histamine (**1**) (100 nM), and ligands were at concentrations from 10 nM to 1 mM; pK_B = −log K_B. [h]Determined in a steady-state [^{32}P]GTPase assay on Sf9 cells expressing the related receptors.

DOI: 10.1021/acsomega.8b00128
ACS Omega 2018, 3, 2865−2882

Table 3. Agonistic Activities of 1, 5, 57, 58, and 63 at the *h*/*gp*/*r*H_2R Determined in the [^{35}S]GTPγS Binding Assay[a]

	hH_2R[b,g]			*gp*H_2R[c]			*r*H_2R[d]		
compound	pEC_{50}[e]	E_{max}[f]	*N*	pEC_{50}[e]	E_{max}[f]	*N*	pEC_{50}[e]	E_{max}[f]	*N*
1	6.01 ± 0.07	1.00	7	5.82 ± 0.02	1.00	3	5.97 ± 0.02	1.00	3
5	6.78 ± 0.01	0.50 ± 0.03	6	7.60 ± 0.02	0.95 ± 0.05	3	7.18 ± 0.07	0.80 ± 0.01	3
57	7.27 ± 0.05	0.52 ± 0.03	6	7.53 ± 0.03	0.89 ± 0.07	3	7.61 ± 0.10	0.80 ± 0.03	3
58	6.61 ± 0.03	0.33 ± 0.03	5	7.28 ± 0.05	0.97 ± 0.06	3	6.83 ± 0.09	0.70 ± 0.04	3
63	6.60 ± 0.02	0.47 ± 0.03	6	7.33 ± 0.03	1.02 ± 0.04	3	6.85 ± 0.07	0.87 ± 0.02	3

[a]Data represent mean values ± SEM from at least three independent experiments (*N*), each performed in triplicate. Data were analyzed by nonlinear regression and were best-fitted to sigmoidal CRCs. [b][^{35}S]GTPγS binding assay at membranes of Sf9 cells expressing the *h*H_2R + $G_s\alpha_s$. [c][^{35}S]GTPγS binding assay at membranes of Sf9 cells expressing the *gp*H_2R + $G_s\alpha_s$. [d][^{35}S]GTPγS binding assay at membranes of Sf9 cells expressing the *r*H_2R + $G_s\alpha_s$. [e]pEC_{50}: $-\log EC_{50}$. [f]E_{max}: maximal response relative to histamine (E_{max} = 1.00). [g]Data taken from Table 2.

Table 4. Agonistic (pEC_{50}) and Antagonistic (pA_2) Activities of 1, 2, 5, 53−63, 127−141, and 145 Determined by Organ Bath Studies at the *gp*H_1R (Ileum) and the *gp*H_2R (Atrium)[a]

	gpH_1R		*gp*H_2R		
compound	pA_2[b] (pEC_{50})	*N*	pEC_{50}[c,d]	E_{max}[e]	*N*
1	(6.68 ± 0.03)	255	6.16 ± 0.01	1.00	225
2	n.a.[f]	24	5.16 ± 0.04	0.75 ± 0.03	5
5	5.77 ± 0.04	9	7.98 ± 0.05	0.91 ± 0.05	3
53	6.20 ± 0.03	9	7.31 ± 0.03	0.96 ± 0.01	3
54	5.89 ± 0.03	9	7.42 ± 0.07	0.94 ± 0.01	3
55	5.69 ± 0.04	9	7.78 ± 0.04	0.90 ± 0.04	3
56	6.64 ± 0.05	8	7.60 ± 0.08	0.71 ± 0.04	3
57	6.91 ± 0.04	9	8.11 ± 0.08	0.63 ± 0.03	3
58	5.88 ± 0.03	9	8.38 ± 0.05	0.78 ± 0.01	3
59	6.08 ± 0.03	9	7.69 ± 0.06	0.94 ± 0.03	3
60	5.37 ± 0.05	9	5.31 ± 0.06	0.20 ± 0.02	3
61	5.85 ± 0.04	6	7.99 ± 0.05	0.91 ± 0.03	3
62	6.01 ± 0.05	6	8.25 ± 0.06	1.02 ± 0.06	3
63	6.00 ± 0.04	6	8.56 ± 0.06	0.88 ± 0.03	3
127	4.23 ± 0.02	4	5.10 ± 0.06	0.58 ± 0.07	3
128	5.08 ± 0.03	10	5.14 ± 0.05	0.55 ± 0.07	3
129	4.83 ± 0.05	8	5.40 ± 0.11	0.83 ± 0.03	3
130	5.27 ± 0.04	10	5.81 ± 0.08	0.87 ± 0.04	3
131	5.39 ± 0.04	11	6.08 ± 0.12	0.86 ± 0.04	3
132	4.99 ± 0.03	14	5.87 ± 0.05	0.86 ± 0.08	3
133	n.d.[g]	0	4.82 ± 0.09	0.92 ± 0.03	3
134	5.35 ± 0.04	12	6.44 ± 0.11	0.90 ± 0.02	3
135	5.14 ± 0.03	19	6.62 ± 0.07	0.89 ± 0.05	3
136	6.10 ± 0.06	8	6.71 ± 0.10	1.13 ± 0.07	3
137	6.74 ± 0.05	12	6.53 ± 0.08	0.90 ± 0.03	3
138	6.71 ± 0.05	12	6.63 ± 0.07	0.91 ± 0.03	3
139	6.36 ± 0.06	6	6.57 ± 0.07	0.60 ± 0.02	3
140	6.43 ± 0.07	6	6.25 ± 0.07	0.70 ± 0.01	3
141	6.43 ± 0.06	6	n.a.	0	3
145	5.24 ± 0.04	9	5.82 ± 0.07	1.00 ± 0.03	3

[a]Data represent mean values ± SEM from at least three independent experiments (*N*). Data were analyzed by nonlinear regression and were best-fitted to sigmoidal CRCs. [b]pA_2: $-\log c(\text{Ant}) + \log(r-1)$; $r = 10^{\Delta pEC_{50}}$; ΔpEC_{50} was calculated from pEC_{50} of histamine and pEC_{50} of histamine in the presence of the respective antagonist. [c]pEC_{50}: $-\log EC_{50}$. [d]pEC_{50} was calculated from the mean-corrected shift ΔpEC_{50} of the agonist curve relative to the histamine reference curve by equation $pEC_{50} = 6.16 + \Delta pEC_{50}$. [e]$E_{max}$: maximal response relative to the maximal increase in heart rate induced by histamine (E_{max} = 1.00). [f]n.a. = not active. [g]n.d. = not determined.

hH_2R (maximum deviation less than 1 log unit). Monomeric imidazole-type compounds with small side chains, like **129**, showing high *h*H_4R affinity, could be of interest for the development of selective *h*H_4R ligands to play an important role in different inflammatory, allergic, and immunological processes.[34,35] Molecular modeling studies, including the bivalent ligands **5** and **58**, suggested an interaction of the guanidine groups with the acidic residues D98$^{3.32}$ and D186$^{5.42}$ as key contributions to H_2R binding. As the bisalkylguanidines turned out to be very stable chemical entities, the synthesized H_2R selective aminothiazole derivatives represent promising lead structures for the development of pharmacological tools for the H_2R, such as **58**, **59**, and **63**. Moreover, the presented data could be of interest for the development of CNS penetrating H_2R agonists—in consideration of changing the basicity of the strongly basic alkylguanidine structure, using

DOI: 10.1021/acsomega.8b00128
ACS Omega 2018, 3, 2865−2882

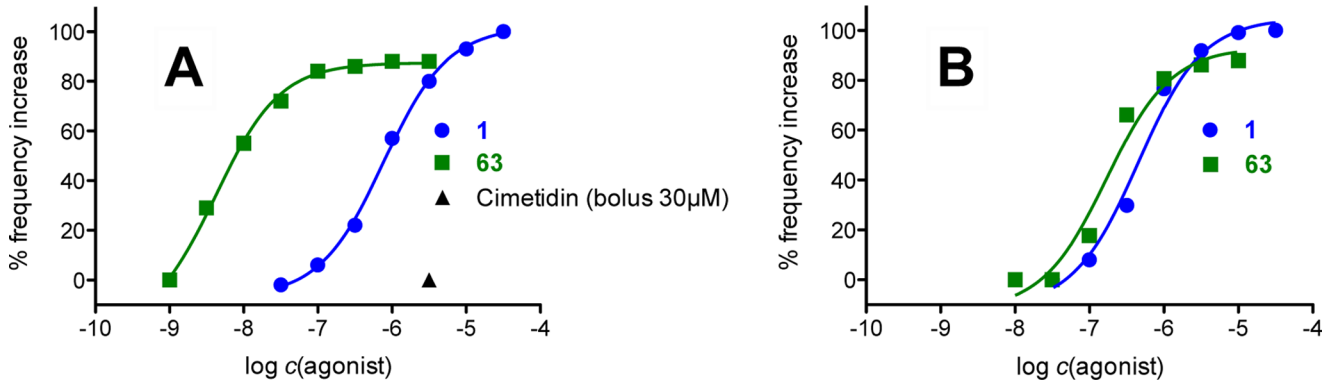

Figure 5. CRCs of histamine (reference) and **63** in the absence (A) and presence (B) of 30 μM cimetidine at the *gp*H_2R (atrium). Displayed curves were calculated by endpoint determination (N = 1).

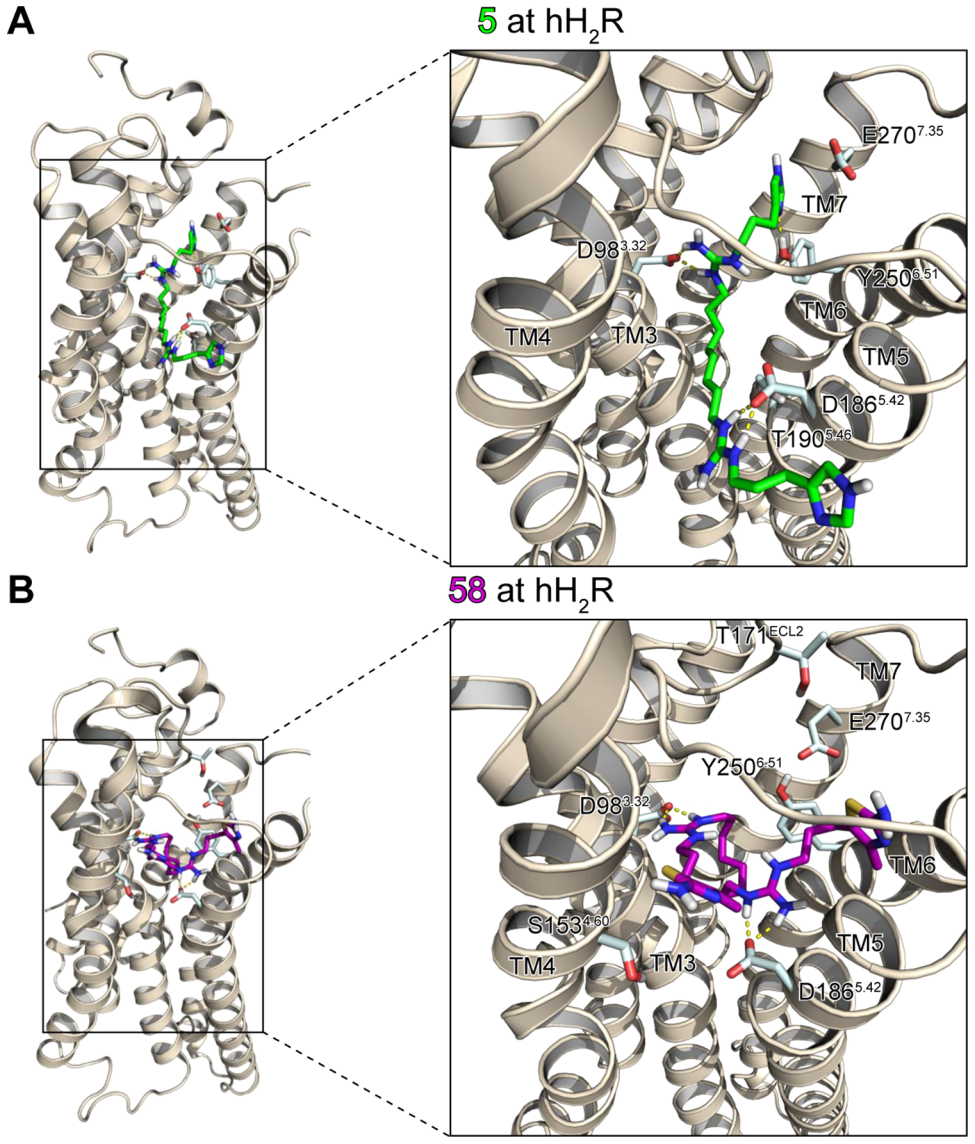

Figure 6. Most probable binding mode of **5** (A) and **58** (B) at the *h*H_2R, showing the respective most predominant clustered structure with the lowest binding free energy of the docking poses investigated by 30 ns MD simulations. Fundamental amino acids involved in ligand binding are shown as light-blue sticks, **5** is colored in green and **58** in magenta. H-bond contacts are illustrated as dashed yellow lines. The allosteric binding site is located most likely between ECL2 and ECL3.

bioisosteric approaches, and the lipophilicity—and H_2R ligands useful for the treatment of acute myeloid leukemia.

DOI: 10.1021/acsomega.8b00128
ACS Omega 2018, 3, 2865−2882

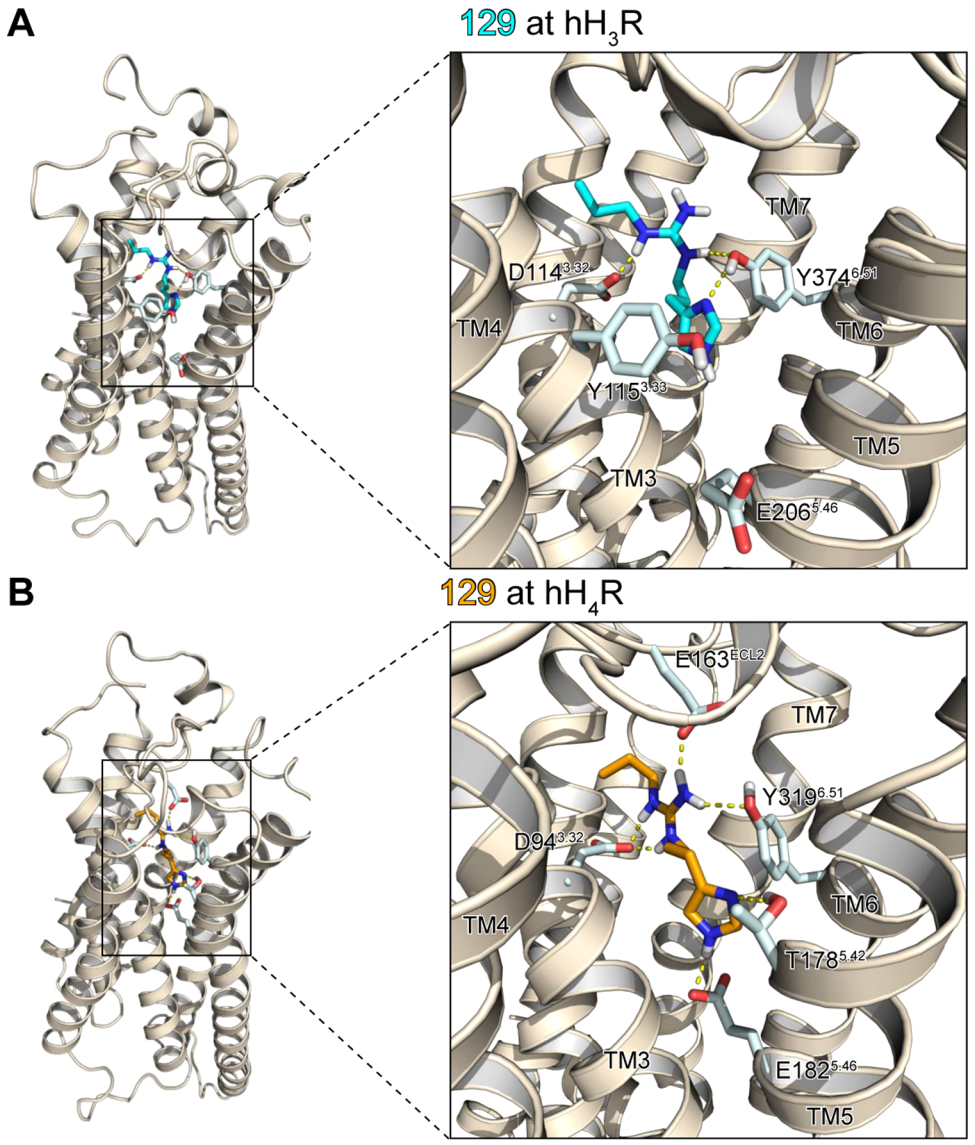

Figure 7. Most probable binding modes of **129** at both the *h*H_3R (A) and *h*H_4R (B), showing the respective most predominant clustered structure with the lowest binding free energy of the docking poses investigated by 30 ns MD simulations. Fundamental amino acids involved in ligand binding are shown as light-blue sticks, **129** is colored in cyan when bound to the *h*H_3R (A) and in orange when bound to the *h*H_4R (B). H-bond contacts are illustrated as dashed yellow lines. The allosteric binding site is located most likely between ECL2 and ECL3 in both cases.

4. EXPERIMENTAL SECTION

4.1. General Conditions. Commercially available chemicals (**9**, **10**, **11**−**16**, **64**−**69**, and **82**−**87**) and solvents were purchased from Acros Organics (Geel, Belgium), Alfa Aesar GmbH & Co. KG (Karlsruhe, Germany), Iris Biotech GmbH (Marktredwitz, Germany), Merck KGaA (Darmstadt, Germany), Sigma-Aldrich Chemie GmbH (München, Germany), or TCI Europe (Zwijndrecht, Belgium) and were used as received. Deuterated solvents for nuclear magnetic resonance (^{1}H NMR and ^{13}C NMR) spectra were purchased from Deutero GmbH (Kastellaun, Germany). Compounds **6**−**8** were prepared as previously described.[22,32,36,37] The synthesis steps described in Section 2.1 were carried out according to reported procedures.[8,17−19] All reactions involving dry solvents were accomplished in dry flasks under nitrogen or argon atmosphere. Millipore water was used for the preparation of buffers, HPLC eluents, and stock solutions. Column chromatography was carried out using Merck silica gel Geduran 60 (0.063−0.200 mm) or Merck silica gel 60 (0.040−0.063 mm) (flash column chromatography). The reactions were monitored by thin-layer chromatography (TLC) on Merck silica gel 60 F_{254} aluminum sheets, and spots were visualized under UV light at 254 nm, by iodine vapor, ninhydrin, or fast blue B staining.

Nuclear magnetic resonance (^{1}H NMR and ^{13}C NMR) spectra were recorded on a Bruker (Karlsruhe, Germany) Avance 300 (^{1}H: 300 MHz, ^{13}C: 75 MHz) or Avance 400 (^{1}H: 400 MHz, ^{13}C: 101 MHz) spectrometer using perdeuterated solvents. The chemical shift δ is given in parts per million (ppm). Multiplicities were specified with the following abbreviations: s (singlet), d (doublet), t (triplet), q (quartet), quint (quintet), m (multiplet), and br (broad signal) as well as combinations thereof. ^{13}C NMR peaks were determined by distortionless enhancement by polarization transfer (DEPT) 135 and DEPT 90: "+" primary and tertiary carbon atom (positive DEPT 135 signal), "−" secondary carbon atom (negative DEPT 135 signal), and "quat" quaternary carbon atom. NMR spectra were processed with MestReNova 11.0

DOI: 10.1021/acsomega.8b00128
ACS Omega 2018, 3, 2865−2882

(Mestrelab Research, Compostela, Spain). High-resolution mass spectrometry (HRMS) was performed on an Agilent 6540 UHD Accurate-Mass quadrupole time-of-flight liquid chromatography/mass spectrometry (MS) system (Agilent Technologies, Santa Clara, CA) using an electrospray ionization (ESI) source. Elemental analyses (EA) were performed on a Heraeus Elementar Vario EL III and are within ±0.4% unless otherwise noted. Melting points (mp) were measured on a Büchi (Essen, Germany) B-545 apparatus using an open capillary and are uncorrected. Preparative HPLC was performed with a system from Knauer (Berlin, Germany) consisting of two K-1800 pumps and a K-2001 detector. A Eurospher-100 C18 (250 × 32 mm^2, 5 μm) (Knauer, Berlin, Germany) or a Kinetex XB-C18 (250 × 21.2 mm^2, 5 μm) (Phenomenex, Aschaffenburg, Germany) served as stationary phase. As mobile phase, 0.1% TFA in millipore water and acetonitrile (MeCN) were used. The temperature was 25 °C, the flow rate was 15 mL/min, and UV detection was performed at 220 nm. Analytical HPLC was performed on system from Merck-Hitachi (Darmstadt/Düsseldorf, Germany) composed of an L-6200-A pump, an AS 2000A autosampler, an L-4000A UV detector, and a D-6000 interface. Stationary phase was a Eurosphere-110 C18 (250 × 4 mm^2, 5 μm) (Knauer, Berlin, Germany) or a Kinetex XB-C18 (250 × 4.6 mm^2, 5 μm) (Phenomenex, Aschaffenburg, Germany). As mobile phase, mixtures of MeCN and aqueous TFA were used (linear gradient: MeCN/TFA (0.1%) (v/v) 0 min: 5:95, 25 min: 50:50, 26−35 min: 95:5 (method A); 0 min: 10:90, 25 min: 50:50, 26−35 min: 95:5 (method B); flow rate = 0.80 mL/min, t_0 = 3.32 min). Capacity factors were calculated according to $k = (t_R - t_0)/t_0$. Detection was performed at 220 nm. All compounds were analyzed using method A, except for **139**−**141** (method B). Furthermore, filtration of the stock solutions with poly(tetrafluoroethylene) filters (25 mm, 0.2 μm, Phenomenex Ltd., Aschaffenburg, Germany) was accomplished before testing. Compound purities determined by HPLC were calculated as the peak area of the analyzed compound in % relative to the total peak area (UV detection at 220 nm). The HPLC purities (see Supporting Information) of the final compounds were ≥95% except for compound **58** (94.3%). The tested compounds were screened for pan-assay interference compounds (PAINS) and aggregation by publicly available filters (http://zinc15.docking.org/patterns/home, http://advisor.docking.org).[38,39] None of the screened structures have been previously reported as PAINS or an aggregator. Since Devine et al. described 2-aminothiazoles as a promiscuous frequent hitting scaffold at different enzymes,[40] full dose−response curves for all experiments and compounds, not only for the 2-aminothiazoles, were measured. None of the curves showed abnormalities, e.g., high Hill slopes, which could be a hint for PAINS.[39]

4.2. Chemical Synthesis and Analytical Data.

*4.2.1. General Procedure for the Synthesis of the Dibenzoylthioureas **17**−**22**.* To an ice-cold solution of the pertinent diamine (**11**−**16**, 1 equiv) in dichloromethane (DCM), benzoyl isothiocyanate (2 equiv) in DCM was added dropwise. The reaction was allowed to stir at room temperature (rt) overnight, and the organic solvent was concentrated under vacuum. The residue was suspended in 80 mL of methanol (MeOH) for 1 h and filtered to give the pure title compound.

*4.2.1.1. N,N′-{[Octane-1,8-diylbis(azanediyl)]bis-[carbonothioyl]}dibenzamide (**20**).* The title compound was prepared from octane-1,8-diamine (**14**, 1.08 g, 7.50 mmol) and **10** (2.02 mL, 15.00 mmol) in DCM (30 mL) according to the general procedure (R_f = 0.40 in ethyl acetate (EtOAc)/Hex 1:3). The product was obtained as a yellow solid (3.30 g, 93%), mp 146.8 °C. ^{1}H NMR (300 MHz, $CDCl_3$) δ (ppm) 10.74 (brs, 2H), 9.00 (brs, 2H), 7.88−7.78 (m, 4H), 7.68−7.57 (m, 2H), 7.56−7.45 (m, 4H), 3.71 (q, J = 7.2 Hz, 4H), 1.72 (quint, J = 6.7 Hz, 4H), 1.54−1.29 (m, 8H). ^{13}C NMR (75 MHz, $CDCl_3$) δ (ppm) 179.7, 166.9, 133.6, 131.8, 129.2, 127.4, 45.9, 29.1, 28.2, 26.8. HRMS (ESI-MS): m/z [M + H^+] calculated for $C_{24}H_{31}N_4O_2S_2^+$: 471.1883, found 471.1884, $C_{24}H_{30}N_4O_2S_2$ (470.65).

*4.2.2. General Procedure for the Synthesis of the Bisthioureas **23**−**28**.* The corresponding dibenzoylthiourea (**17**−**22**, 1 equiv) was stirred in a solution of K_2CO_3 (4.1 equiv) in MeOH/H_2O (7/3 v/v) for 3−5 h at rt. The proportion of MeOH was evaporated, and the resulting suspension was stirred for 1 h. The pure product was filtered with a Büchner funnel.

Because of the thione−thiol tautomerism, a splitting of the NH−C***H***$_2$−$(CH_2)_x$−C***H***$_2$−NH signal could be observed in the following NMR spectra. Two broad singlets could be noted right next to each other. In each case, the integration value was exactly 4. For all of the other symmetric CH_2 peaks, this peak splitting was not shown.

*4.2.2.1. 1,1′-(Octane-1,8-diyl)bis(thiourea) (**26**).*[41] The title compound was prepared from **20** (3.30 g, 7.01 mmol) and K_2CO_3 (3.88 g, 28.75 mmol) in MeOH/H_2O (7/3 v/v, 100 mL) according to the general procedure (R_f = 0.43 in DCM/MeOH/NH_3 90:10:0.1), yielding a colorless solid (1.80 g, 98%), mp 187.2 °C. ^{1}H NMR (300 MHz, dimethyl sulfoxide (DMSO)-d_6) δ (ppm) 7.60 (brs, 2H), 6.88 (brs, 4H), 3.32 + 3.00 (2 brs, 2.4H + 1.6H (thione−thiol tautomerism)), 1.43 (quint, J = 6.9 Hz, 4H), 1.31−1.20 (m, 8H). ^{13}C NMR (75 MHz, DMSO-d_6) δ (ppm) 182.9, 41.3, 32.7, 28.7, 26.2. HRMS (ESI-MS): m/z [M + H^+] calculated for $C_{10}H_{23}N_4S_2^+$: 263.1359, found 263.1359; $C_{10}H_{22}N_4S_2$ (262.44).

*4.2.3. General Procedure for the Synthesis of the Bis-S-methylisothioureas (**29**−**34**).* The appropriate bisthiourea (**23**−**28**, 1 equiv) was dissolved in 50 mL of acetonitrile (MeCN) and treated with methyl iodide (2.1 equiv). The reaction mixture was stirred for 1 h under refluxing and the solvent was evaporated under vacuum. The resulting product (di-HI salt) was washed three times with 20 mL of diethylether (Et_2O) and dried under vacuum.

*4.2.3.1. 1,1′-(Octane-1,8-diyl)bis(S-methylisothiourea) (**32**).* The compound **26** (1.80 g, 6.86 mmol) was dissolved in MeCN (50 mL) and treated with methyl iodide (0.90 mL, 14.40 mmol) according to the general procedure (R_f = 0.16 in DCM/MeOH/NH_3 90:10:0.1). The resulting product was obtained as a yellow oil (**32**·2HI, 3.70 g, 99%). ^{1}H NMR (300 MHz, CD_3OD, hydrogen iodide) δ (ppm) 3.38 (t, J = 7.2 Hz, 4H), 2.65 (s, 6H), 1.66 (quint, J = 7.2 Hz, 4H), 1.44−1.36 (m, 8H). ^{13}C NMR (75 MHz, CD_3OD, hydrogen iodide) δ (ppm) 170.0, 45.5, 30.2, 29.0, 27.7, 14.4. HRMS (ESI-MS): m/z [M + H^+] calculated for $C_{12}H_{27}N_4S_2^+$: 291.1672, found 291.1674; $C_{12}H_{26}N_4S_2$·2HI (546.32).

*4.2.4. General Procedure for the Synthesis of the Bis-N′-boc-S-methylisothioureas (**35**−**40**).* To a solution of the pertinent isothiourea (**29**−**34**) and 2 equiv of triethylamine (NEt_3) in 50 mL of DCM, a solution of Boc_2O (2 equiv) in 20 mL of DCM was added dropwise at rt. The reaction mixture was stirred overnight (rt) and washed with H_2O and a saturated

DOI: 10.1021/acsomega.8b00128
ACS Omega 2018, 3, 2865−2882

solution of NaCl. The organic layer was dried over Na_2SO_4, and the crude product was purified by column chromatography (EtOAc/petroleum ether (PE) 1/4−1/2 v/v).

*4.2.4.1. 1,1′-(Octane-1,8-diyl)bis(N′-tert-butoxycarbonyl-S-methylisothiourea) (**38**).* The reaction was carried out with **32** (3.70 g, 6.77 mmol), NEt_3 (1.88 mL, 13.55 mmol), and Boc_2O (2.96 g, 13.55 mmol) according to the general procedure (R_f = 0.62 in EtOAc/Hex 1:2), yielding a colorless oil (3.30 g, 99%). ^{1}H NMR (300 MHz, $CDCl_3$) δ (ppm) 9.56 (brs, 2H), 3.28 (q, J = 7.0 Hz, 4H), 2.45 (s, 6H), 1.65−1.56 (m, 4H), 1.49 (s, 18H), 1.38−1.30 (m, 8H). ^{13}C NMR (75 MHz, $CDCl_3$) δ (ppm) 173.5, 162.3, 79.2, 43.8, 29.3, 29.0, 28.3, 26.7, 13.6. HRMS (ESI-MS): m/z [M + H^+] calculated for $C_{22}H_{43}N_4O_4S_2^+$: 491.2720, found 491.2721; $C_{22}H_{42}N_4O_4S_2$ (490.72).

*4.2.5. General Procedure for the Guanidinylation Reaction of **41**−**49**.* To a suspension of the corresponding amine **6**, **7**, **8**, or **9** (2 equiv), the pertinent bis-N′-boc-S-methylisothiourea **35**−**40** (1 equiv), and $HgCl_2$ (2 equiv) in DCM, NEt_3 (6 equiv) was added. The mixture was stirred overnight at rt. A possible excess of $HgCl_2$ was quenched with 7 N NH_3 in MeOH (3−5 mL). The resulting suspension was filtered over Celite, and the crude product was purified by column chromatography (DCM/MeOH/7 N NH_3 in MeOH 98/1/1−95/3/2 v/v/v).

*4.2.5.1. 1,1′-(Octane-1,8-diyl)bis{N″-tert-butoxycarbonyl-N′-[3-(1-trityl-1H-imidazol-4-yl)propyl]guanidine} (**44**).* The title compound was synthesized from **6** (500 mg, 1.36 mmol), **38** (334 mg, 0.68 mmol), $HgCl_2$ (369 mg, 1.36 mmol), and NEt_3 (0.57 mL, 4.08 mmol) in DCM (20 mL) according to the general procedure (R_f = 0.27 in DCM/MeOH/NH_3 98:2:0.1). The product was obtained as a yellow oil (460 mg, 60%). ^{1}H NMR (300 MHz, $CDCl_3$) δ (ppm) 9.05 (brs, 2H), 7.38−7.19 (m, 20H), 7.15−7.01 (m, 12H), 6.53 (d, J = 1.4 Hz, 2H), 3.46−3.02 (m, 8H), 2.55 (t, J = 6.4 Hz, 4H), 1.84 (quint, J = 6.8 Hz, 4H), 1.44 (m + s, 4 + 18H), 1.22−1.12 (m, 8H). ^{13}C NMR (75 MHz, $CDCl_3$) δ (ppm) 164.4, 160.5, 142.3, 140.6, 138.0, 129.7, 128.1, 128.1, 118.3, 77.5, 75.2, 41.4, 40.7, 29.2, 28.8, 28.7, 28.6, 26.9. HRMS (ESI-MS): m/z [M + H^+] calculated for $C_{70}H_{85}N_{10}O_4^+$: 1129.6750, found 1129.6737; $C_{70}H_{84}N_{10}O_4$ (1129.51).

*4.2.5.2. 1,1′-(Octane-1,8-diyl)bis{N″-tert-butoxycarbonyl-N′-[(2-tert-butoxycarbonyl-amino-4-methylthiazol-5-yl)-propyl]guanidine} (**47**).* The title compound was synthesized from **7** (554 mg, 2.04 mmol), **38** (500 mg, 1.02 mmol), $HgCl_2$ (554 mg, 2.04 mmol), and NEt_3 (0.85 mL, 6.12 mmol) in DCM (20 mL) according to the general procedure (R_f = 0.28 in DCM/MeOH/NH_3 98:2:0.1). The product was obtained as a yellow foamlike solid (520 mg, 54%). ^{1}H NMR (300 MHz, $CDCl_3$) δ (ppm) 11.28 (brs, 2H), 3.24−3.06 (m, 8H), 2.67 (t, J = 6.5 Hz, 4H), 2.17 (s, 6H), 1.82 (quint, J = 7.3 Hz, 4H), 1.44 (s, 18H), 1.39 (m + s, 4 + 18H), 1.23−1.16 (m, 8H). ^{13}C NMR (75 MHz, $CDCl_3$) δ (ppm) 164.2, 160.0, 158.3, 152.9, 142.1, 122.9, 82.2, 77.9, 41.1, 40.3, 30.7, 29.1, 29.0, 28.4, 28.3, 26.7, 23.3, 14.5. HRMS (ESI-MS): m/z [M + H^+] calculated for $C_{44}H_{77}N_{10}O_8S_2^+$: 937.5362, found 937.5367; $C_{44}H_{76}N_{10}O_8S_2$ (937.27).

*4.2.6. General Procedure for the Guanidinylation Reaction of **50**−**52**.* To a suspension of the corresponding amine **6**, **7**, or **8** (two out of them, each 1 equiv), **38** (1 equiv), and $HgCl_2$ (2 equiv) in DCM, NEt_3 (6 equiv) was added. The mixture was stirred overnight at rt. A possible excess of $HgCl_2$ was quenched with 7 N NH_3 in MeOH (3−5 mL). The resulting suspension was filtered over Celite, and the crude product was used in the next step without further purification.

*4.2.6.1. 2-tert-Butoxycarbonyl-1-[3-(2-tert-butoxycarbonyl-amino-4-methylthiazol-5-yl)propyl]-3-{8-[2-tert-butoxycarbonyl-3-(3-(2-tert-butoxycarbonylaminothiazol-5-yl)-propyl)guanidino]octyl}guanidine (**52**).* The title compound was synthesized from **7** (111 mg, 0.41 mmol), **8** (105 mg, 0.41 mmol), **38** (200 mg, 0.41 mmol), $HgCl_2$ (222 mg, 0.82 mmol), and NEt_3 (0.17 mL, 1.22 mmol) in DCM (20 mL) according to the general procedure. The crude product was used in the next step without further purification. HRMS (ESI-MS): m/z [M + H^+] calculated for $C_{43}H_{75}N_{10}O_8S_2^+$: 923.5204, found 923.5208; $C_{43}H_{74}N_{10}O_8S_2$ (923.25).

*4.2.7. General Procedure for the Synthesis of the Bivalent Ligands (**5** and **53**−**63**).* TFA (4.0 mL) was added to a solution of the protected precursors **41**−**52** in DCM (16.0 mL, 20% TFA in DCM), and the mixture was refluxed overnight until the protecting groups were removed (TLC control). Subsequently, the solvent was evaporated in vacuo and the residue was washed three times with Et_2O (each 20 mL). The crude product was purified by preparative RP-HPLC (MeCN/0.1% TFA (aq): 5/95−40/60). All compounds were dried by lyophilization and obtained as tetra-trifluoroacetates.

*4.2.7.1. 1,1′-(Octane-1,8-diyl)bis{3-[3-(1H-imidazol-4-yl)-propyl]guanidine} (**5**).*[13] Prepared from **44** (280 mg, 0.25 mmol) in DCM (16.0 mL) and TFA (4.0 mL) according to the general procedure, **5** was yielded as a yellow oil (150 mg, 67%): RP-HPLC: 98%, (t_R = 13.97, k = 3.21). ^{1}H NMR (300 MHz, CD_3OD, tetra-trifluoroacetate) δ (ppm) 8.83 (d, J = 1.2 Hz, 2H), 7.39 (s, 2H), 3.28 (t, J = 7.5 Hz, 4H), 3.20 (t, J = 7.0 Hz, 4H), 2.83 (t, J = 7.8 Hz, 4H), 1.98 (quint, J = 7.4 Hz, 4H), 1.59 (quint, J = 6.9 Hz, 4H), 1.42−1.35 (m, 8H). ^{13}C NMR (75 MHz, CD_3OD, tetra-trifluoroacetate) δ (ppm) 163.1 (q, J = 35.2 Hz), 157.6, 154.3, 134.9, 134.5, 117.1, 42.7, 41.7, 30.3, 30.0, 28.9, 27.7, 22.6. HRMS (ESI-MS): m/z [M + H^+] calculated for $C_{22}H_{41}N_{10}^+$: 445.3510, found 445.3506; $C_{22}H_{40}N_{10}$·4TFA (900.72).

*4.2.7.2. 1,1′-(Dodecane-1,12-diyl)bis{3-[3-(1H-imidazol-4-yl)propyl]guanidine} (**57**).* Prepared from **46** (240 mg, 0.20 mmol) in DCM (16.0 mL) and TFA (4.0 mL) according to the general procedure, **57** was yielded as a yellow oil (120 mg, 62%): RP-HPLC: 99%, (t_R = 17.84, k = 4.37). ^{1}H NMR (300 MHz, CD_3OD, tetra-trifluoroacetate) δ (ppm) 8.77 (d, J = 1.3 Hz, 2H), 7.32 (d, J = 0.9 Hz, 2H), 3.27 (t, J = 7.0 Hz, 4H), 3.17 (t, J = 7.1 Hz, 4H), 2.80 (t, J = 7.7 Hz, 4H), 1.95 (quint, J = 7.3 Hz, 4H), 1.56 (quint, J = 6.8 Hz, 4H), 1.34−1.26 (m, 16H). ^{13}C NMR (75 MHz, CD_3OD, tetra-trifluoroacetate) δ (ppm) 163.1 (q, J = 34.8 Hz), 157.6, 157.6, 134.8, 134.6, 129.0 (q, J = 44.3 Hz), 117.0, 42.7, 41.6, 30.7, 30.7, 30.4, 30.0, 28.9, 27.8, 22.6. HRMS (ESI-MS): m/z [M + H^+] calculated for $C_{26}H_{49}N_{10}^+$: 501.4136, found 501.4131; $C_{26}H_{48}N_{10}$·4TFA (956.83).

*4.2.7.3. 1,1′-(Octane-1,8-diyl)bis{3-[3-(2-amino-4-methyl-thiazol-5-yl)propyl]guanidine} (**58**).* Prepared from **47** (520 mg, 0.55 mmol) in DCM (16.0 mL) and TFA (4.0 mL) according to the general procedure, **58** was yielded as a yellow oil (280 mg, 51%): RP-HPLC: 94%, (t_R = 15.53, k = 3.68). ^{1}H NMR (300 MHz, CD_3OD, tetra-trifluoroacetate) δ (ppm) 3.26−3.10 (m, 8H), 2.71 (t, J = 7.1 Hz, 4H), 2.20 (s, 6H), 1.86 (quint, J = 7.3 Hz, 4H), 1.61−1.52 (m, 4H), 1.37−1.30 (m, 8H). ^{13}C NMR (75 MHz, CD_3OD, tetra-trifluoroacetate) δ (ppm) 170.4, 162.8 (q, J = 35.6 Hz), 157.6, 157.6, 132.4, 118.5, 42.6, 41.5, 30.6, 30.2, 29.9, 27.7, 23.5, 11.5. HRMS (ESI-MS):

DOI: 10.1021/acsomega.8b00128
ACS Omega 2018, 3, 2865−2882

m/z [M + H^+] calculated for $C_{24}H_{45}N_{10}S_2^+$: 537.3265, found 537.3261; $C_{24}H_{44}N_{10}S_2$·4TFA (992.90).

*4.2.7.4. 1-[3-(2-Amino-4-methylthiazol-5-yl)propyl]-3-{8-[3-(3-(2-aminothiazol-5-yl)propyl)guanidino]octyl}guanidine (**63**).* Prepared from **53** (without purification) in DCM (16.0 mL) and TFA (4.0 mL) according to the general procedure, **63** was yielded as a yellow oil (28.3 mg, 7.1%): RP-HPLC: 95%, (t_R = 15.87, k = 3.78). ^{1}H NMR (300 MHz, CD_3OD, tetra-trifluoroacetate) δ (ppm) 7.02 (s, 1H), 3.29−3.05 (m, 8H), 2.85−2.55 (m, 4H), 2.19 (s, 3H), 2.00−1.73 (m, 4H), 1.69−1.50 (m, 4H), 1.46−1.30 (m, 8H). ^{13}C NMR (75 MHz, CD_3OD, tetra-trifluoroacetate) δ (ppm) 171.7, 170.3, 157.5, 132.4, 126.7, 123.7, 118.9, 43.1, 42.0, 41.9, 31.0, 30.8, 30.4, 30.2, 27.9, 25.3, 24.0, 12.4. HRMS (ESI-MS): m/z [M + H^+] calculated for $C_{23}H_{43}N_{10}S_2^+$: 523.3108, found 523.3106; $C_{23}H_{42}N_{10}S_2$·4TFA (978.87).

*4.2.8. General Procedure for the Synthesis of the Benzoylthioureas **70**−**75**.* To an ice-cold solution of the pertinent amine (**64**−**69**, 1 equiv) in MeCN, benzoyl isothiocyanate (1 equiv) was added dropwise. The reaction was stirred at room temperature (rt) for 2 h, and the organic solvent was concentrated under vacuum. The residue was dissolved in DCM (50 mL) and washed three times with H_2O and saturated solution of NaCl. The organic layer was dried over Na_2SO_4, and the crude product was purified by column chromatography (EtOAc/PE 1/9−1/6 v/v).

*4.2.8.1. N-(Isobutylcarbamothioyl)benzamide (**70**).*[42] The title compound was prepared from isobutylamine (**64**, 1.00 mL, 10.00 mmol) and **10** (1.34 mL, 10.00 mmol) in MeCN (30 mL) according to the general procedure (R_f = 0.41 in EtOAc/Hex 1:7). The product was obtained as a beige-colored solid (2.10 g, 89%), mp 79.6 °C. ^{1}H NMR (300 MHz, $CDCl_3$) δ (ppm) 10.83 (brs, 1H), 8.98 (brs, 1H), 7.88−7.80 (m, 2H), 7.67−7.59 (m, 1H), 7.56−7.48 (m, 2H), 3.55 (td, J = 6.9, 5.4 Hz, 2H), 2.06 (m, 1H), 1.03 (d, J = 6.7 Hz, 6H). ^{13}C NMR (75 MHz, $CDCl_3$) δ (ppm) 179.85, 166.90, 133.59, 131.81, 129.19, 127.41, 53.38, 27.61, 20.29. HRMS (ESI-MS): m/z [M + H^+] calculated for $C_{12}H_{17}N_2OS^+$: 237.1056, found 237.1057; $C_{12}H_{16}N_2OS$ (236.33).

*4.2.9. General Procedure for the Synthesis of the Thioureas **76**−**81**.* The corresponding benzoylthiourea (**70**−**75**, 1 equiv) was stirred in a solution of K_2CO_3 (2.1 equiv) in MeOH/H_2O (7/3 v/v) for 3−5 h at rt. The proportion of MeOH was evaporated, and the resulting suspension was extracted with DCM and stirred for 1 h. The organic layer was dried over Na_2SO_4, and the crude product was purified by column chromatography (DCM/MeOH/7M NH_3 in MeOH 95/3/2 v/v).

Because of the thione−thiol tautomerism, a splitting of the NH−C***H***$_2$−R-signal could be observed in the following NMR spectra. Two broad singlets could be noted right next to each other. In each case, the integration value was exactly 2. For all of the other symmetric CH_2 peaks, this peak splitting was not shown.

4.2.9.1. N-Isobutylthiourea (76).[42] The title compound was prepared from **70** (2.00 g, 8.46 mmol) and K_2CO_3 (2.46 g, 17.77 mmol) in MeOH/H_2O (7/3 v/v, 50 mL) according to the general procedure (R_f = 0.38 in DCM/MeOH/NH_3 95:5:0.1), yielding a colorless oil (0.78 g, 70%). ^{1}H NMR (300 MHz, $CDCl_3$) δ (ppm) 6.96 (brs, 1H), 6.32 (brs, 2H), 3.34 + 2.93 (2 brs, 0.9H + 1.1H (thione−thiol tautomerism)), 1.88 (m, 1H), 0.94 (d, J = 6.6 Hz, 6H). ^{13}C NMR (75 MHz, $CDCl_3$) δ (ppm) 180.76, 51.82, 27.85, 20.23. HRMS (ESI-MS): m/z [M + H^+] calculated for $C_5H_{13}N_2S^+$: 133.0794, found 133.0794; $C_5H_{12}N_2S$ (132.23).

*4.2.10. General Procedure for the Synthesis of the S-Methylisothioureas (**88**−**99**).* The appropriate thiourea (**76**−**87**, 1 equiv) was dissolved in 30 mL of MeCN and treated with methyl iodide (1.1 equiv). The reaction mixture was stirred for 1 h under refluxing, and the solvent was evaporated under vacuum. The resulting product (HI salt) was washed three times with 20 mL of diethylether (Et_2O) and dried under vacuum.

*4.2.10.1. S-Methyl-N-propylisothiourea (**90**).*[43] The compound **84** (1.18 g, 10.00 mmol) was dissolved in MeCN (30 mL) and treated with methyl iodide (0.69 mL, 11.00 mmol) according to the general procedure (R_f = 0.41 in DCM/MeOH/NH_3 90:10:0.1). The resulting product was obtained as an orange oil (**90**·HI, 2.50 g, 96%). ^{1}H NMR (300 MHz, $CDCl_3$, hydrogen iodide) δ (ppm) 3.30 (t, J = 7.1 Hz, 2H), 2.79 (s, 3H), 1.74 (m, 2H), 1.03 (t, J = 7.4 Hz, 3H). ^{13}C NMR (75 MHz, $CDCl_3$, hydrogen iodide) δ (ppm) 170.49, 46.60, 21.93, 15.28, 11.45. HRMS (ESI-MS): m/z [M + H^+] calculated for $C_5H_{12}N_2S^+$: 133.0794, found 133.0796; $C_5H_{12}N_2S$·HI (260.14).

*4.2.11. General Procedure for the Synthesis of the N′-Boc-S-methylisothioureas (**100**−**111**).* To a solution of the pertinent isothiourea (**88**−**99**) and 1 equiv of triethylamine (NEt_3) in 50 mL of DCM, a solution of Boc_2O (1 equiv) in 20 mL of DCM was added dropwise at rt. The reaction mixture was stirred overnight (rt) and washed with H_2O and saturated solution of NaCl. The organic layer was dried over Na_2SO_4, and the crude product was purified by column chromatography (EtOAc/PE 1/9−1/5 v/v).

*4.2.11.1. N′-tert-Butoxycarbonyl-S-methyl-N-propylisothiourea (**102**).* The reaction was carried out with **90** (2.46 g, 9.46 mmol), NEt_3 (1.31 mL, 9.46 mmol), and Boc_2O (2.06 g, 9.46 mmol) according to the general procedure (R_f = 0.50 in EtOAc/Hex 1:8), yielding a colorless oil (1.74 g, 79%). ^{1}H NMR (300 MHz, $CDCl_3$) δ (ppm) 9.81 (brs, 1H), 3.26 (q, J = 7.3 Hz, 2H), 2.45 (s, 3H), 1.64 (m, 2H), 1.49 (s, 9H), 0.96 (t, J = 7.4 Hz, 3H). ^{13}C NMR (75 MHz, $CDCl_3$) δ (ppm) 173.44, 162.27, 79.17, 45.52, 28.25, 22.65, 13.56, 11.39. HRMS (ESI-MS): m/z [M + H^+] calculated for $C_{10}H_{21}N_2O_2S^+$: 233.1318, found 233.1321; $C_{10}H_{20}N_2O_2S$ (232.34).

*4.2.12. General Procedure for the Guanidinylation Reaction of **112**−**126** and **144**.* To a suspension of the corresponding amine **6**, **7**, **8**, or **9** (1 equiv), the pertinent *N′*-boc-*S*-methylisothiourea **100**−**111** or **143** (1 equiv), and $HgCl_2$ (2 equiv) in DCM, NEt_3 (3 equiv) was added. The mixture was stirred overnight at rt. A possible excess of $HgCl_2$ was quenched with 7 N NH_3 in MeOH (3−5 mL). The resulting suspension was filtered over Celite, and the crude product was purified by column chromatography (DCM/MeOH/7 N NH_3 in MeOH 98/1/1−95/3/2 v/v/v).

*4.2.12.1. 2-tert-Butoxycarbonyl-1-propyl-3-[3-(1-trityl-1H-imidazol-4-yl)propyl]guanidine (**114**).* The title compound was synthesized from **6** (808 mg, 2.20 mmol), **102** (510 mg, 2.20 mmol), $HgCl_2$ (1.19 g, 4.40 mmol), and NEt_3 (0.91 mL, 6.60 mmol) in DCM (20 mL) according to the general procedure (R_f = 0.24 in DCM/MeOH/NH_3 98:2:0.1). The product was obtained as a yellow foamlike solid (620 mg, 51%). ^{1}H NMR (300 MHz, $CDCl_3$) δ (ppm) 9.05 (brs, 1H), 7.39−7.21 (m, 10H), 7.16−7.04 (m, 6H), 6.54 (s, 1H), 3.56−2.95 (m, 4H), 2.57 (t, J = 6.2 Hz, 2H), 1.86 (quint, J = 6.6 Hz, 2H), 1.51 (m, 2H), 1.47 (s, 9H), 0.83 (t, J = 7.4 Hz, 3H). ^{13}C NMR

DOI: 10.1021/acsomega.8b00128
ACS Omega 2018, 3, 2865−2882

(75 MHz, $CDCl_3$) δ (ppm) 164.49, 160.52, 142.38, 140.67, 138.07, 129.73, 128.34, 128.06, 118.25, 75.20, 53.49, 43.03, 40.67, 29.63, 28.69, 28.57, 22.52, 11.53. HRMS (ESI-MS): m/z [M + H^+] calculated for $C_{34}H_{42}N_5O_2^+$: 552.3333, found 552.3338; $C_{34}H_{41}N_5O_2$ (551.74).

*4.2.13. General Procedure for the Synthesis of the Monomeric Ligands (**127**−**141** and **145**).* TFA (4.0 mL) was added to a solution of the protected precursors **112**−**126** or **144** in DCM (16.0 mL, 20% TFA in DCM), and the mixture was refluxed overnight until the protecting groups were removed (TLC control). Subsequently, the solvent was evaporated in vacuo and the residue was washed three times with Et_2O (each 20 mL). The crude product was purified by preparative RP-HPLC (MeCN/0.1% TFA (aq): 5/95−40/60). All compounds were dried by lyophilization and obtained as di-trifluoroacetates.

*4.2.13.1. 1-[3-(1H-Imidazol-4-yl)propyl]-3-propylguanidine (**129**).*[44] Prepared from **114** (450 mg, 0.82 mmol) in DCM (16.0 mL) and TFA (4.0 mL) according to the general procedure, **129** was yielded as a beige-colored solid (310 mg, 87%), mp 126.7 °C. ^{1}H NMR (300 MHz, CD_3OD, di-trifluoroacetate) δ (ppm) 8.80 (d, J = 1.3 Hz, 1H), 7.34 (s, 1H), 3.26 (t, J = 7.0 Hz, 2H), 3.15 (t, J = 7.1 Hz, 2H), 2.80 (t, J = 7.2 Hz, 2H), 1.96 (quint, J = 7.3 Hz, 2H), 1.61 (m, 2H), 0.97 (t, J = 7.4 Hz, 3H). ^{13}C NMR (75 MHz, CD_3OD, di-trifluoroacetate) δ (ppm) 157.58, 134.92, 134.57, 116.97, 44.27, 41.58, 28.82, 23.25, 22.56, 11.41. HRMS (ESI-MS): m/z [M + H^+] calculated for $C_{10}H_{20}N_5^+$: 210.1713, found 210.1714; $C_{10}H_{19}N_5$·2TFA (437.34).

*4.2.14. Synthesis of Di-tert-butyl-2-thioxodihydropyrimidin-1,3(2H,4H)-dicarboxylat (**143**).*[45] To a stirred solution of **142** (871 mg, 7.50 mmol) in THF (150 mL) under argon at 0 °C, hexane (20 mL) and sodium hydride (1.35 g, 33.8 mmol, 60% in mineral oil) were added. After 5 min, the ice bath was removed, and the reaction mixture was stirred at room temperature for 10 min. The mixture was cooled to 0 °C again, di-*tert*-butyl dicarbonate (3.60 g, 16.5 mmol) was added, and the ice bath was removed after 30 min of stirring at that temperature. The resulting slurry was stirred for another 2 h at room temperature. Then, the reaction was quenched with an aqueous solution of saturated $NaHCO_3$ (10 mL). The reaction mixture was poured into water (250 mL) and extracted with EtOAc (3 × 70 mL). The combined organic layer was dried over Na_2SO_4, filtered, and concentrated in vacuo to give **143** as a yellow solid (1.88 g, 79%), mp 84.7 °C. ^{1}H NMR (300 MHz, $CDCl_3$) δ (ppm) 3.67 (t, J = 6.9 Hz, 4H), 2.15 (quint, J = 6.9 Hz, 2H), 1.53 (s, 18H). ^{13}C NMR (75 MHz, $CDCl_3$) δ (ppm) 182.68, 153.66, 84.09, 44.26, 27.77, 24.02. HRMS (ESI-MS): m/z [M + H^+] calculated for $C_{14}H_{25}N_2O_4S^+$: 317.1530, found 317.1532; $C_{14}H_{24}N_2O_4S$ (316.42).

4.3. Pharmacological Methods. *4.3.1. Materials.* Histamine dihydrochloride was purchased from Alfa Aesar GmbH & Co. KG (Karlsruhe, Germany). [^{3}H]mepyramine (specific activity: 20.0 Ci/mmol), [^{3}H]tiotidine (specific activity: 78.4 Ci/mmol), [^{3}H]N^α-methylhistamine (specific activity: 85.3 Ci/mmol), and [^{3}H]histamine (specific activity: 25.0 Ci/mmol) were obtained from Hartmann Analytic (Braunschweig, Germany). GTPγS was purchased from Roche (Mannheim, Germany), and [^{35}S]GTPγS was purchased from PerkinElmer Life Science (Boston) or Hartmann Analytic (Braunschweig, Germany). [^{3}H]UR-DE257 was synthesized in our laboratories. All stock solutions were dissolved in millipore water or in a mixture of Millipore water/DMSO. In all assays, the final DMSO content amounted to <0.5%.

4.3.2. Membrane Preparations.[46] Sf9 cells were seeded at 3.0 × 10^6 cells/mL and infected with a 1:100 dilution of high-titer baculovirus stocks encoding hH$_1$R + RGS4, h/gp/r H$_2$R + G$_s\alpha_s$, hH$_3$R G$_i\alpha_2$ + G$\beta_1\gamma_2$, or hH$_4$R G$_i\alpha_2$ + G$\beta_1\gamma_2$. The cells were cultured for 48 h before the production of the membrane preparation according to a previously reported protocol, using 1 mM ethylenediaminetetraacetic acid (EDTA), 0.2 mM phenylmethylsulfonyl fluoride, 10 μg/mL benzamidine, and 10 μg/mL leupeptin as protease inhibitors. Membranes were suspended in binding buffer (12.5 mM $MgCl_2$, 1 mM EDTA, and 75 mM Tris/HCl, pH 7.4) and stored at −80 °C until use.

4.3.3. Radioligand Binding Assay.[14,47−49] Sf9 membranes were thawed and sedimented by centrifugation at 13 000g at 4 °C for 10 min. The membranes (hH$_1$R + RGS4, hH$_2$R + G$_s\alpha_s$, hH$_3$R G$_i\alpha_2$ + G$\beta_1\gamma_2$, hH$_4$R G$_i\alpha_2$ + G$\beta_1\gamma_2$) were resuspended in a cold (4 °C) binding buffer (BB: 12.5 mM $MgCl_2$, 1 mM EDTA, and 75 mM Tris/HCl, pH 7.4) at a final soluble protein concentration of 2−6 μg per 1 μL BB. Experiments were performed in 96-well plates (polypropylene (PP) microplates 96 well, Greiner Bio-One, Frickenhausen, Germany) using a total volume of 100 μL of BB, which contained 40−90 μg of membrane, 0.05% bovine serum albumin (BSA), the respective radioligand ([^{3}H]mepyramine 5 nM, [^{3}H]tiotidine 10 nM, [^{3}H] UR-DE257 20 nM, [^{3}H]N^α-methylhistamine 3 nM, or [^{3}H]histamine 15 nM), and the investigated ligands at various concentrations. During the incubation period (60 min) at room temperature, the plates were shaken at 250 rpm with a Heidolph Titramax 101 (Heidolph Instruments GmbH & Co. KG, Schwabach, Germany). Afterward, bound radioligand was separated from free radioligand by collection of the membranes on polyethylenimine-pretreated GF/C filters (Whatman, Maidstone, U.K.) using a 96-well Brandel harvester (Brandel Inc., Unterföhring, Germany). After two washing steps with binding buffer, filter pieces were punched and transferred into 1450-401 96-well sample plates (PerkinElmer, Rodgau, Germany). Scintillation cocktail (200 μL, Rotiszint Eco plus, Roth, Karlsruhe, Germany) was added, and the plates were sealed with Plateseal 1450-461 (PerkinElmer, Rodgau, Germany) and incubated in the dark for 12 h. Radioactivity (dpm) was measured with a MicroBeta^2 1450 scintillation counter (PerkinElmer). Experimental data were analyzed by nonlinear regression and were best-fitted to sigmoidal concentration−response curves using Prism 5.0c software (GraphPad, San Diego, CA).[50]

4.3.4. [^{35}S]GTPγS Binding Assay.[14,49,51,52] Membranes of Sf9 cells expressing the h/gp/rH$_2$R + G$_s\alpha_s$, hH$_3$R G$_i\alpha_2$ + G$\beta_1\gamma_2$, or hH$_4$R G$_i\alpha_2$ + G$\beta_1\gamma_2$ were thawed and sedimented by centrifugation at 13 000g at 4 °C for 10 min. The membranes were resuspended in a cold (4 °C) binding buffer BB (12.5 mM $MgCl_2$, 1 mM EDTA, and 75 mM Tris/HCl, pH 7.4) at a final soluble protein concentration of 1 μg per 1 μL BB. All H$_4$R experiments contained additionally 100 mM NaCl. For investigations in the antagonist mode, histamine was added to the reaction mixture (hH$_2$R: 1 μM, hH$_{3,4}$R: 100 nM). Experiments were performed in 96-well plates (PP microplates 96 well, Greiner Bio-One, Frickenhausen, Germany) in a total volume of 100 μL, containing 10 μg of membrane, 1 μM GDP, 0.05% BSA, 20 nCi [^{35}S]GTPγS, and the investigated ligands at various concentrations. During the incubation period (90 min) at room temperature, the plates were shaken at 250 rpm with a Heidolph Titramax 101 (Heidolph Instruments GmbH & Co.

DOI: 10.1021/acsomega.8b00128
ACS Omega 2018, 3, 2865−2882

KG, Schwabach, Germany). Afterward, bound radioligand was separated from free radioligand by filtration through GF/C filters (Whatman, Maidstone, U.K.) using a 96-well Brandel harvester (Brandel Inc., Unterföhring, Germany). After two washing steps with binding buffer, the filter pieces were punched and transferred into 1450-401 96-well sample plates (PerkinElmer). Unspecific binding was determined in the presence of 10 μM GTPγS. Each well was supplemented with 200 μL of scintillation cocktail (Rotiszint Eco plus, Roth, Karlsruhe, Germany), and the plates were sealed with Plateseal 1450-461 (PerkinElmer, Rodgau, Germany) and incubated in the dark for 12 h. Radioactivity (ccpm) was measured with a MicroBeta^2 1450 scintillation counter (PerkinElmer). Data were analyzed by nonlinear regression and were best-fitted to sigmoidal concentration−response curves with the Prism 5.0c software (GraphPad, San Diego, CA).

4.3.5. Histamine H_1 Receptor Assay on Isolated Guinea Pig Ileum.[15] Guinea pigs of either sex (250−500 g) were stunned by a blow on the neck and exsanguinated. The ileum was rapidly removed, rinsed, and cut into segments of 1.5−2.0 cm length. The tissues were mounted isotonically (preload of 5 mN) in a jacketed 20 mL organ bath that was filled with Tyrode's solution (composition [mM]: NaCl, 137; KCl, 2.7; $CaCl_2$, 1.8; $MgCl_2$, 1.0; NaH_2PO_4, 0.4; $NaHCO_3$, 11.9; and glucose 5.0) supplemented with atropine, at a concentration not affecting H_1 receptors (0.05 μM), to block cholinergic muscarinic receptors. The bath was aerated with 95% O_2/5% CO_2 and heated to 37 °C. During an equilibration period of 80 min, the tissues were stimulated three times with histamine (2 × 1 μM, 1 × 10 μM) followed by washout. Up to four cumulative CRCs were determined on each tissue: the first by addition of histamine (0.01−30 μM) and the second to fourth by addition of histamine in the presence of increasing concentrations of antagonist (preincubation: 10−15 min). pEC_{50} differences were not corrected because four successive curves for histamine were superimposable under these conditions (N > 10). Data were analyzed by nonlinear regression and were best-fitted to sigmoidal concentration−response curves using Prism 5.0c software (GraphPad, San Diego, CA).

4.3.6. Histamine H_2 Receptor Assay on the Isolated Guinea Pig Right Atrium (Spontaneously Beating).[2,16,53] Hearts were rapidly removed from guinea pigs used for studies on the ileum (see above). The right atrium was quickly dissected and set up isometrically in the Krebs−Henseleit solution under a diastolic resting force of approximately 5 mN in a jacketed 20 mL organ bath at 32.5 °C. The bath fluid (composition [mM]: NaCl, 118.1; KCl, 4.7; $CaCl_2$, 1.8; $MgSO_4$, 1.64; KH_2PO_4, 1.2; $NaHCO_3$, 25.0; glucose, 5.0; sodium pyruvate, 2.0), supplemented with (*RS*)-propranolol (0.3 μM) to block β-adrenergic receptors, was equilibrated with 95% O_2 and 5% CO_2. Experiments were started after 30 min of continuous washing and an additional equilibration period of 15 min. Two successive histamine CRCs displayed a significant desensitization of 0.13 ± 0.02 (N = 16 control organs). This value was used to correct each individual experiment. For agonists, two successive concentration−frequency curves were generated: the first for histamine (0.1−30 μM) and the second for the agonist of interest either in the absence or in the presence of cimetidine (30 μM, 30 min preincubated). Additionally, the sensitivity to 30, 100, or 300 μM cimetidine was checked at the end of each H_2R agonist CRC, and a significant reduction of frequency was observed. The relative potency of the agonist under study was calculated from the corrected pEC_{50} difference (ΔpEC_{50}). pEC_{50} values are given relative to the long-term mean value for histamine (pEC_{50} = 6.16) determined in our laboratory (pEC_{50} = 6.16 + ΔpEC_{50}). Data were analyzed by nonlinear regression and were best-fitted to sigmoidal concentration−response curves using Prism 5.0c software (GraphPad, San Diego, CA).

4.4. Computational Methods. *4.4.1. Model Preparation.* To examine possible binding modes of the bivalent ligands **5** and **58** at hH$_2$R and of the monovalent ligand **129** at both hH$_3$R and hH$_4$R, homology models of these receptors were prepared as follows: For hH$_4$R, the described hH$_4$R model was used,[54] which was based on the inactive state crystal structure of the hH$_1$R[55] (PDB ID: 3RZE), and the models comprising hH$_2$R and hH$_3$R were adapted from this model. Model preparation was essentially performed as described in Wifling et al.[54] using the modeling suite SYBYL-X 2.0 (Tripos Inc., St. Louis, MO).

4.4.2. Molecular Docking. The most interesting bivalent compounds **5** and **58** on the one hand and the monomeric ligand **129** on the other hand were geometry-optimized by means of Gaussian 09[56] at the HF/6-31(d,p) level, attributing the ligands a formal charge of +2 and +1, respectively. Upon file conversion by means of Open Babel[57] and assignment of physiological ionization states by means of ChemAxon (http://www.chemaxon.com) Marvin 16.3.28.0, 2016 Calculator Plugins, flexible docking was performed with the software package Autodock Vina.[58] The following hH$_2$R amino acids were kept as flexible: K18, S75, Q79, Y94, T95, D98, V99, C102, R161, N168, H169, T170, T171, S172, K173, K175, V176, V178, N179, E180, G183, D186, G187, T190, W247, Y250, F251, F254, R257, R260, N266, E267, E270, L274, W275, G277, Y278. For hH$_3$R, the amino acids T34, M41, Y91, Y94, V95, W110, L111, D114, Y115, C118, E185, H187, F192, F193, Y194, W196, L199, A202, S203, E206, W371, Y374, T375, M378, R381, H387, D391, D394, E395, D398, W399, L401, W402 were kept as flexible, and for hH$_4$R the residues R15, M22, Y72, H75, T76, W90, L91, D94, Y95, C98, M150, K158, E160, S162, E163, F168, F169, S170, W172, L175, T178, S179, E182, W316, Y319, S320, T323, L326, S330, S331, T333, S337, Y340, R341, F344, W345, Q347, W348. The search box was set to a size of 28 Å × 32 Å × 32 Å, centered at the binding pocket. Up to 20 binding poses were exported for each ligand. Taking into account the results of the scoring function as well as experimental data, the respective best poses were selected for downstream molecular dynamics simulations.

4.4.3. Molecular Dynamics Simulations. To identify the respective most probable binding pose, 30 ns molecular dynamics simulations were performed in a water box at 310 K, and subsequently, free energy (MM-GBSA[59]) calculations were performed using the Amber 14[60] molecular dynamics package. To determine ligand force-field parameters, RESP[61] charges were determined by means of Gaussian 09[56] at the HF/6-31(d,p) level, and general amber force field[62] atom types as well as RESP[61] charges were assigned using antechamber.[60] parmchk2[60] and tleap[60] were used for input file generation. For ligand guanidine atoms and protein residues, the Amber ff99SB[63] force-field parameters were used. The simulation steps were carried out in an octahedral box comprising an 8.0 Å TIP3P[64] water layer and neutralizing chloride ions.[65] The mbondi2 parameter set was utilized.[66,67] The respective systems were minimized using the steepest descent (2500 steps) and conjugated gradient (7500 steps) methods without restraints,

DOI: 10.1021/acsomega.8b00128
ACS Omega 2018, 3, 2865−2882

and were subsequently heated from 0 to 100 K over 50 ps in the NVT ensemble as well as from 100 to 310 K over 450 ps in the NPT ensemble. During the first ns of the 5 ns equilibration period, initial harmonic restraints of 5 kcal/mol Å^2 were applied to all ligand and receptor atoms, and, beginning from 1 ns, harmonic restraints on receptor main chain atoms were reduced from 5.0 to 0.5 kcal/mol Å^2 in a stepwise manner and maintained during the 30 ns simulation. Bonds involving hydrogen atoms were constrained using SHAKE[68] to enable a frame step size of 2 fs.[65,69] Nonbonded interactions were cut off at 8.0 Å, and long-range electrostatics were computed using the particle-mesh Ewald[70] method. The Langevin thermostat[71,72] with a collision frequency of 1.0 ps^{-1} and randomly assigned initial velocities was used to maintain a target temperature of 310 K. The Berendsen barostat[73] with isotropic position scaling and a pressure relaxation time of 1.0 ps was employed to keep the pressure constant at 1 bar. Data were collected every 10 ps. H-bond and cluster analysis were performed by means of CPPTRAJ[60] for the entire 30 ns trajectories. Moreover, the average linkage algorithm[74] was applied for cluster analysis, setting a cluster size of 5, and the programming language R[75−78] was used for the preparation of H-bond plots. Binding free-energy (MM-GBSA) calculations of the 30 ns trajectories were performed using MMPBSA.py[59] and a frame step size of 10 ps, and the corresponding plots were obtained using the Prism 5.01 software (GraphPad, San Diego, CA). All other figures were created with PyMOL Molecular Graphics system, version 1.8.2.1 (Schrödinger LLC, Portland, OR).

■ ASSOCIATED CONTENT

Supporting Information

The Supporting Information is available free of charge on the ACS Publications website at DOI: 10.1021/acsomega.8b00128.

Synthesis and analytical data of compounds **17**−**19**, **21**−**25**, **27**−**31**, **33**−**37**, **39**−**43**, **45**−**46**, **48**−**51**, **53**−**56**, **59**−**62**, **71**−**75**, **77**−**81**, **88**−**89**, **91**−**101**, **103**−**113**, **115**−**128**, **130**−**141**, and **144**−**145**; RP-HPLC images and elemental analyses (purity control) of the target compounds; ^{1}H and ^{13}C NMR spectra of **5**, **57**, **58**, **63**, and **129**; guinea pig right atrium experiments in the presence of cimetidine; and computational data and figures (free energy of binding, cluster analysis) (PDF)

SMILES (XLSX)

■ AUTHOR INFORMATION

Corresponding Author

*E-mail: steffen.pockes@ur.de. Phone: (+49)941-9434814. Fax: (+49)941-9434809.

ORCID

Steffen Pockes: 0000-0002-2211-9868

Max Keller: 0000-0002-8095-8627

Armin Buschauer: 0000-0002-9709-1433

Notes

The authors declare no competing financial interest.

■ ACKNOWLEDGMENTS

The authors thank Christine Braun, Kerstin Röhrl, and Maria Beer-Krön for expert technical assistance. Furthermore, special thanks go to Tim Clark and Jonas Kaindl for providing infrastructure and scientific expertize.

■ DEDICATION

†This paper is dedicated to Prof. Dr. Armin Buschauer, in memoriam (died on July 18, 2017).

■ ABBREVIATIONS

BB, binding buffer; Boc_2O, di-*tert*-butyl carbonate; br, broad signal; CRC, concentration−response curve; **DPH**, diphenhydramine; ECL, extracellular loop; E_{max}, efficacy; ESI, electrospray ionization; ESI-MS, electrospray ionization mass spectrometry; EtOAc, ethyl acetate; GBSA, generalized born surface area; $G_i\alpha_2$, α2-subunit of the G_i protein; *gp*H_1R, *guinea pig* histamine H_1 receptor; *gp*H_2R, *guinea pig* histamine H_2 receptor; $G_s\alpha_s$, α-subunit (short splice variant) of the G_s protein; $G\beta_1\gamma_2$, G-protein β1- and γ2-subunit; GTPγS, guanosine 5′-*O*-[γ-thio]triphosphate; H_2R, histamine H_2 receptor; Hex, hexane; *h*H_1R, *human* histamine H_1 receptor; *h*H_2R, *human* histamine H_2 receptor; *h*H_3R, *human* histamine H_3 receptor; *h*H_4R, *human* histamine H_4 receptor; *h*HR, *human* histamine receptor; K_B, dissociation constant of a antagonist−receptor complex; m, multiplet; MeCN, acetonitrile; MeOH, methanol; MM-GBSA, molecular mechanics generalized born surface area; PE, petroleum ether; pEC_{50}, negative decadic logarithm of EC_{50}; pK_B, negative decadic logarithm of K_B; pK_i, negative decadic logarithm of K_i; RGS4, regulator of G-protein signaling proteins; *r*H_2R, *rat* histamine H_2 receptor; RP-HPLC, reversed-phase HPLC; SEM, standard error of mean; Trt, trityl

■ REFERENCES

(1) Ash, A. S. F.; Schild, H. O. Receptors Mediating Some Actions of Histamine. *Br. J. Pharmacol. Chemother.* **1966**, *27*, 427−439.

(2) Black, J. W.; Duncan, W. A. M.; Durant, C. J.; Ganellin, C. R.; Parsons, E. M. Definition and Antagonism of Histamine H_2-Receptors. *Nature* **1972**, *236*, 385−390.

(3) Arrang, J.-M.; Garbarg, M.; Schwartz, J.-C. Auto-Inhibition of Brain Histamine Release Mediated by a Novel Class (H_3) of Histamine Receptor. *Nature* **1983**, *302*, 832−837.

(4) Oda, T.; Morikawa, N.; Saito, Y.; Masuho, Y.; Matsumoto, S.i. Molecular Cloning and Characterization of a Novel Type of Histamine Receptor Preferentially Expressed in Leukocytes. *J. Biol. Chem.* **2000**, *275*, 36781−36786.

(5) Windaus, A.; Vogt, W. Synthesis of Imidazolylethylamine. *Ber. Dtsch. Chem. Ges.* **1907**, *40*, 3685−3691.

(6) Lagerström, M. C.; Schiöth, H. B. Structural Diversity of G Protein-Coupled Receptors and Significance for Drug Discovery. *Nat. Rev. Drug Discov.* **2008**, *7*, 339−357.

(7) Parsons, M. E.; Blakemore, R. C.; Durant, G. J.; Ganellin, C. R.; Rasmussen, A. C. 3-[4(5)-Imidazolyl] Propylguanidine (SK&F 91486)—a Partial Agonist at Histamine H_2-Receptors. *Agents Actions* **1975**, *5*, 464.

(8) Buschauer, A. Synthesis and in Vitro Pharmacology of Arpromidine and Related Phenyl(pyridylalkyl)guanidines, a Potential New Class of Positive Inotropic Drugs. *J. Med. Chem.* **1989**, *32*, 1963−1970.

(9) Birnkammer, T.; Spickenreither, A.; Brunskole, I.; Lopuch, M.; Kagermeier, N.; Bernhardt, G.; Dove, S.; Seifert, R.; Elz, S.; Buschauer, A. The Bivalent Ligand Approach Leads to Highly Potent and Selective Acylguanidine-Type Histamine H_2 Receptor Agonists. *J. Med. Chem.* **2012**, *55*, 1147−1160.

(10) Kagermeier, N.; Werner, K.; Keller, M.; Baumeister, P.; Bernhardt, G.; Seifert, R.; Buschauer, A. Dimeric Carbamoylguanidine-Type Histamine H_2 Receptor Ligands: A New Class of Potent and Selective Agonists. *Bioorg. Med. Chem.* **2015**, *23*, 3957−3969.

(11) Fukushima, Y.; Asano, T.; Saitoh, T.; Anai, M.; Funaki, M.; Ogihara, T.; Katagiri, H.; Matsuhashi, N.; Yazaki, Y.; Sugano, K. Oligomer Formation of Histamine H_2 Receptors Expressed in Sf9 and COS7 Cells. *FEBS Lett.* **1997**, *409*, 283−286.

DOI: 10.1021/acsomega.8b00128
ACS Omega 2018, 3, 2865−2882

(12) Portoghese, P. S. From Models to Molecules: Opioid Receptor Dimers, Bivalent Ligands, and Selective Opioid Receptor Probes. *J. Med. Chem.* **2001**, *44*, 2259−2269.
(13) Sterk, G. J.; Kramer, K.; van der Goot, H.; Timmerman, H. Studies on Histaminergic Compounds, Part VII. 1 Histamine H_2-Binding on Guinea-Pig Cerebral Cortex Compared to Histamine (ANT) Agonism. *J. Recept. Res.* **1989**, *9*, 417−427.
(14) Kelley, M. T.; Bürckstümmer, T.; Wenzel-Seifert, K.; Dove, S.; Buschauer, A.; Seifert, R. Distinct Interaction of Human and Guinea Pig Histamine H_2-Receptor with Guanidine-Type Agonists. *Mol. Pharmacol.* **2001**, *60*, 1210−1225.
(15) Elz, S.; Kramer, K.; Pertz, H. H.; Detert, H.; ter Laak, A. M.; Kühne, R.; Schunack, W. Histaprodifens: Synthesis, Pharmacological in Vitro Evaluation, and Molecular Modeling of a New Class of Highly Active and Selective Histamine H_1-Receptor Agonists. *J. Med. Chem.* **2000**, *43*, 1071−1084.
(16) Kunze, M. Histamin-H1-Rezeptoragonisten vom Suprahistaprodifen- und 2-Phenylhistamin-Typ und 2-substituierte Imidazolylpropan-Derivate als Liganden für H1/H2/H3/H4-Rezeptoren. Neue Synthesestrategien und pharmakologische Testung. Doctoral Thesis, University of Regensburg: Regensburg, Germany, 2006, https://epub.uni-regensburg.de/10517/.
(17) Frennesson, D. B.; Langley, D. R.; Saulnier, M. G.; Vyas, D. M. Methods for Preparing Macrocycles and Macrocycle Stabilized Peptides. Patent WO2012051405A1, 2012.
(18) Brückner, R. *Reaktionsmechanismen: Organische Reaktionen, Stereochemie, Moderne Synthesemethoden*, 3rd ed.; Springer Spektrum: Berlin, 2004; pp 1−863.
(19) Kim, K. S.; Qian, L. Improved Method for the Preparation of Guanidines. *Tetrahedron Lett.* **1993**, *34*, 7677−7680.
(20) Expósito, A.; Fernández-Suárez, M.; Iglesias, T.; Muñoz, L.; Riguera, R. Total Synthesis and Absolute Configuration of Minalemine A, a Guanidine Peptide from the Marine Tunicate *Didemnum rodriguesi*. *J. Org. Chem.* **2001**, *66*, 4206−4213.
(21) Baumeister, P.; Erdmann, D.; Biselli, S.; Kagermeier, N.; Elz, S.; Bernhardt, G.; Buschauer, A. [^{3}H]UR-DE257: Development of a Tritium-Labeled Squaramide-Type Selective Histamine H_2 Receptor Antagonist. *ChemMedChem* **2015**, *10*, 83−93.
(22) Kraus, A.; Ghorai, P.; Birnkammer, T.; Schnell, D.; Elz, S.; Seifert, R.; Dove, S.; Bernhardt, G.; Buschauer, A. N^G-Acylated Aminothiazolylpropylguanidines as Potent and Selective Histamine H_2 Receptor Agonists. *ChemMedChem* **2009**, *4*, 232−240.
(23) Pertz, H. H.; Görnemann, T.; Schurad, B.; Seifert, R.; Straßer, A. Striking Differences of Action of Lisuride Stereoisomers at Histamine H_1 Receptors. *Naunyn-Schmiedeberg's Arch. Pharmacol.* **2006**, *374*, 215−222.
(24) Igel, P.; Schneider, E.; Schnell, D.; Elz, S.; Seifert, R.; Buschauer, A. N^G-Acylated Imidazolylpropylguanidines as Potent Histamine H_4 Receptor Agonists: Selectivity by Variation of the N^G-Substituent. *J. Med. Chem.* **2009**, *52*, 2623−2627.
(25) Brimblecombe, R. W.; Duncan, W. A. M.; Durant, G. J.; Emmett, J. C.; Ganellin, C. R.; Parsons, M. E. Cimetidine—a Non-Thiourea H_2-Receptor Antagonist. *J. Int. Med. Res.* **1975**, *3*, 86−92.
(26) Brimblecombe, R. W.; Duncan, W. A. M.; Durant, G. J.; Ganellin, C. R.; Parsons, M. E.; Black, J. W. Proceedings: The Pharmacology of Cimetidine, a New Histamine H_2-Receptor Antagonist. *Br. J. Pharmacol.* **1975**, *53*, 435−436.
(27) Shi, L.; Javitch, J. A. The Binding Site of Aminergic G Protein-Coupled Receptors: The Transmembrane Segments and Second Extracellular Loop. *Annu. Rev. Pharmacol. Toxicol.* **2002**, *42*, 437−467.
(28) Jongejan, A.; Lim, H. D.; Smits, R. A.; de Esch, I. J.; Haaksma, E.; Leurs, R. Delineation of Agonist Binding to the Human Histamine H_4 Receptor Using Mutational Analysis, Homology Modeling, and Ab Initio Calculations. *J. Chem. Inf. Model.* **2008**, *48*, 1455−1463.
(29) Shin, N.; Coates, E.; Murgolo, N. J.; Morse, K. L.; Bayne, M.; Strader, C. D.; Monsma, F. J. Molecular Modeling and Site-Specific Mutagenesis of the Histamine-Binding Site of the Histamine H_4 Receptor. *Mol. Pharmacol.* **2002**, *62*, 38−47.
(30) Schultes, S.; Nijmeijer, S.; Engelhardt, H.; Kooistra, A. J.; Vischer, H. F.; de Esch, I. J. P.; Haaksma, E. E. J.; Leurs, R.; de Graaf, C. Mapping Histamine H_4 Receptor-Ligand Binding Modes. *Med. Chem. Commun.* **2013**, *4*, 193−204.
(31) Gantz, I.; DelValle, J.; Wang, L. D.; Tashiro, T.; Munzert, G.; Guo, Y. J.; Konda, Y.; Yamada, T. Molecular Basis for the Interaction of Histamine with the Histamine H_2 Receptor. *J. Biol. Chem.* **1992**, *267*, 20840−20843.
(32) Eriks, J. C.; Van der Goot, H.; Sterk, G. J.; Timmerman, H. Histamine H_2-Receptor Agonists. Synthesis, in Vitro Pharmacology, and Qualitative Structure−Activity Relationships of Substituted 4- and 5-(2-Aminoethyl)thiazoles. *J. Med. Chem.* **1992**, *35*, 3239−3246.
(33) Coruzzi, G.; Timmerman, H.; Adami, M.; Bertaccini, G. The New Potent and Selective Histamine H_2 Receptor Agonist Amthamine as a Tool to Study Gastric Secretion. *Naunyn-Schmiedeberg's Arch. Pharmacol.* **1993**, *348*, 77−81.
(34) Lim, H. D.; Smits, R. A.; Leurs, R.; De Esch, I. J. P. The Emerging Role of the Histamine H_4 Receptor in Anti-Inflammatory Therapy. *Curr. Top. Med. Chem.* **2006**, *6*, 1365−1373.
(35) Thurmond, R. L.; Gelfand, E. W.; Dunford, P. J. The Role of Histamine H_1 and H_4 Receptors in Allergic Inflammation: The Search for New Antihistamines. *Nat. Rev. Drug Discovery* **2008**, *7*, 41−53.
(36) Ghorai, P.; Kraus, A.; Keller, M.; Götte, C.; Igel, P.; Schneider, E.; Schnell, D.; Bernhardt, G.; Dove, S.; Zabel, M.; Elz, S.; Seifert, R.; Buschauer, A. Acylguanidines as Bioisosteres of Guanidines: N^G-Acylated Imidazolylpropylguanidines, a New Class of Histamine H_2 Receptor Agonists. *J. Med. Chem.* **2008**, *51*, 7193−7204.
(37) Mitsunobu, O.; Yamada, M.; Mukaiyama, T. Preparation of Esters of Phosphoric Acid by the Reaction of Trivalent Phosphorus Compounds with Diethyl Azodicarboxylate in the Presence of Alcohols. *Bull. Chem. Soc. Jpn.* **1967**, *40*, 935−939.
(38) Baell, J. B.; Holloway, G. A. New Substructure Filters for Removal of Pan Assay Interference Compounds (PAINS) from Screening Libraries and for Their Exclusion in Bioassays. *J. Med. Chem.* **2010**, *53*, 2719−2740.
(39) Aldrich, C.; Bertozzi, C.; Georg, G. I.; Kiessling, L.; Lindsley, C.; Liotta, D.; Merz, K. M.; Schepartz, A.; Wang, S. The Ecstasy and Agony of Assay Interference Compounds. *ACS Cent. Sci.* **2017**, *3*, 143−147.
(40) Devine, S. M.; Mulcair, M. D.; Debono, C. O.; Leung, E. W. W.; Nissink, J. W. M.; Lim, S. S.; Chandrashekaran, I. R.; Vazirani, M.; Mohanty, B.; Simpson, J. S.; Baell, J. B.; Scammells, P. J.; Norton, R. S.; Scanlon, M. J. Promiscuous 2-Aminothiazoles (PrATs): A Frequent Hitting Scaffold. *J. Med. Chem.* **2015**, *58*, 1205−1214.
(41) Kawai, S.; Hosono, T.; Shikinami, Y.; Yonechi, S. Researches on Hypoglycemia Producing Substances. II. Pseudo-Thiourea, Amidine, and Urea Derivatives. *Sci. Pap. Inst. Phys. Chem. Res. (Jpn.)* **1931**, *16*, 9.
(42) Kodomari, M.; Suzuki, M.; Tanigawa, K.; Aoyama, T. A Convenient and Efficient Method for the Synthesis of Mono- and N,N-Disubstituted Thioureas. *Tetrahedron Lett.* **2005**, *46*, 5841−5843.
(43) Schlee, H. G.; Sasse, K.; Eue, L. Tetrahydro-1,3,5-triazine-2,6-diones. Patents US4056527A, 1977.
(44) Elz, S.; Schunack, W. Synthesis and H_2-Agonistic Activity of Alkyl-[3-(4-Imidazolyl)propyl]guanidines. *Arch. Pharm.* **1987**, *320*, 182−185.
(45) Iwama, S.; Kitano, T.; Fukuya, F.; Honda, Y.; Sato, Y.; Notake, M.; Morie, T. Discovery of a Potent and Selective $\alpha_v\beta_3$ Integrin Antagonist with Strong Inhibitory Activity against Neointima Formation in Rat Balloon Injury Model. *Bioorg. Med. Chem. Lett.* **2004**, *14*, 2567−2570.
(46) Schneider, E. H.; Seifert, R. Sf9 Cells: A Versatile Model System to Investigate the Pharmacological Properties of G Protein-Coupled Receptors. *Pharmacol. Ther.* **2010**, *128*, 387−418.
(47) de Jong, L. A. A.; Uges, D. R. A.; Franke, J. P.; Bischoff, R. Receptor−ligand Binding Assays: Technologies and Applications. *J. Chromatogr. B* **2005**, *829*, 1−25.
(48) Seifert, R.; et al. Multiple Differences in Agonist and Antagonist Pharmacology between Human and Guinea Pig Histamine H_1-Receptor. *J. Pharmacol. Exp. Ther.* **2003**, *305*, 1104−1115.

DOI: 10.1021/acsomega.8b00128
ACS Omega 2018, 3, 2865−2882

(49) Schnell, D.; Burleigh, K.; Trick, J.; Seifert, R. No Evidence for Functional Selectivity of Proxyfan at the Human Histamine H_3 Receptor Coupled to Defined G_i/G_o Protein Heterotrimers. *J. Pharmacol. Exp. Ther.* **2010**, *332*, 996−1005.
(50) *GraphPad Prism*, version 5.01; GraphPad Software Inc.: San Diego, CA, 2007, www.graphpad.com.
(51) Schneider, E. H.; Seifert, R. Histamine H_4 receptor−RGS Fusion Proteins Expressed in Sf9 Insect Cells: A Sensitive and Reliable Approach for the Functional Characterization of Histamine H_4 Receptor Ligands. *Biochem. Pharmacol.* **2009**, *78*, 607−616.
(52) Schneider, E. H.; Schnell, D.; Papa, D.; Seifert, R. High Constitutive Activity and a G-Protein-Independent High-Affinity State of the Human Histamine H_4-Receptor. *Biochemistry* **2009**, *48*, 1424−1438.
(53) Lennartz, H.-G.; Hepp, M.; Schunack, W. Synthese Und Wirkung 5-Alkylsubstituierter Histamine Und N^{α}-Methylhistamine. *Eur. J. Med. Chem.* **1978**, *13*, 229−234.
(54) Wifling, D.; Löffel, K.; Nordemann, U.; Strasser, A.; Bernhardt, G.; Dove, S.; Seifert, R.; Buschauer, A. Molecular Determinants for the High Constitutive Activity of the Human Histamine H_4 Receptor: Functional Studies on Orthologues and Mutants. *Br. J. Pharmacol.* **2015**, *172*, 785−798.
(55) Shimamura, T.; Shiroishi, M.; Weyand, S.; Tsujimoto, H.; Winter, G.; Katritch, V.; Abagyan, R.; Cherezov, V.; Liu, W.; Han, G. W.; et al. Structure of the Human Histamine H_1 Receptor Complex with Doxepin. *Nature* **2011**, *475*, 65−70.
(56) Frisch, M. J.; Trucks, G. W.; Schlegel, H. B.; Scuseria, G. E.; Robb, M. A.; Cheeseman, J. R.; Scalmani, G.; Barone, V.; Mennucci, B.; Petersson, G. A. *Gaussian09*, revision D.01; Gaussian Inc.: Wallingford, CT, 2013.
(57) O'Boyle, N. M.; Banck, M.; James, C. A.; Morley, C.; Vandermeersch, T.; Hutchison, G. R. Open Babel: An Open Chemical Toolbox. *J. Cheminf.* **2011**, *3*, 33.
(58) Trott, O.; Olson, A. J. AutoDock Vina: Improving the Speed and Accuracy of Docking with a New Scoring Function, Efficient Optimization, and Multithreading. *J. Comput. Chem.* **2010**, *31*, 455−461.
(59) Miller, B. R., III; McGee, T. D., Jr.; Swails, J. M.; Homeyer, N.; Gohlke, H.; Roitberg, A. E. MMPBSA. Py: An Efficient Program for End-State Free Energy Calculations. *J. Chem. Theory Comput.* **2012**, *8*, 3314−3321.
(60) Case, D. A.; Babin, V.; Berryman, J.; Betz, R. M.; Cai, Q.; Cerutti, D. S.; Cheatham Iii, T. E.; Darden, T. A.; Duke, R. E.; Gohlke, H., et al. *Amber 14*, University of California, San Francisco, 2014, ambermd.org.
(61) Bayly, C. I.; Cieplak, P.; Cornell, W.; Kollman, P. A. A Well-Behaved Electrostatic Potential Based Method Using Charge Restraints for Deriving Atomic Charges: The RESP Model. *J. Phys. Chem.* **1993**, *97*, 10269−10280.
(62) Wang, J.; Wolf, R. M.; Caldwell, J. W.; Kollman, P. A.; Case, D. A. Development and Testing of a General Amber Force Field. *J. Comput. Chem.* **2004**, *25*, 1157−1174.
(63) Hornak, V.; Abel, R.; Okur, A.; Strockbine, B.; Roitberg, A.; Simmerling, C. Comparison of Multiple Amber Force Fields and Development of Improved Protein Backbone Parameters. *Proteins: Struct., Funct., Bioinf.* **2006**, *65*, 712−725.
(64) Jorgensen, W. L.; Chandrasekhar, J.; Madura, J. D.; Impey, R. W.; Klein, M. L. Comparison of Simple Potential Functions for Simulating Liquid Water. *J. Chem. Phys.* **1983**, *79*, 926−935.
(65) Möller, D.; Kling, R. C.; Skultety, M.; Leuner, K.; Hübner, H.; Gmeiner, P. Functionally Selective Dopamine D_2, D_3 Receptor Partial Agonists. *J. Med. Chem.* **2014**, *57*, 4861−4875.
(66) Onufriev, A.; Bashford, D.; Case, D. A. Modification of the Generalized Born Model Suitable for Macromolecules. *J. Phys. Chem. B* **2000**, *104*, 3712−3720.
(67) Onufriev, A.; Bashford, D.; Case, D. A. Exploring Protein Native States and Large-scale Conformational Changes with a Modified Generalized Born Model. *Proteins: Struct., Funct., Bioinf.* **2004**, *55*, 383−394.
(68) Ryckaert, J.-P.; Ciccotti, G.; Berendsen, H. J. C. Numerical Integration of the Cartesian Equations of Motion of a System with Constraints: Molecular Dynamics of N-Alkanes. *J. Comput. Phys.* **1977**, *23*, 327−341.
(69) Pegoli, A.; She, X.; Wifling, D.; Hübner, H.; Bernhardt, G.; Gmeiner, P.; Keller, M. Radiolabeled Dibenzodiazepinone-Type Antagonists Give Evidence of Dualsteric Binding at the M_2 Muscarinic Acetylcholine Receptor. *J. Med. Chem.* **2017**, *60*, 3314−3334.
(70) Darden, T.; York, D.; Pedersen, L. Particle Mesh Ewald: An N·Log (N) Method for Ewald Sums in Large Systems. *J. Chem. Phys.* **1993**, *98*, 10089−10092.
(71) Uberuaga, B. P.; Anghel, M.; Voter, A. F. Synchronization of Trajectories in Canonical Molecular-Dynamics Simulations: Observation, Explanation, and Exploitation. *J. Chem. Phys.* **2004**, *120*, 6363−6374.
(72) Sindhikara, D. J.; Kim, S.; Voter, A. F.; Roitberg, A. E. Bad Seeds Sprout Perilous Dynamics: Stochastic Thermostat Induced Trajectory Synchronization in Biomolecules. *J. Chem. Theory Comput.* **2009**, *5*, 1624−1631.
(73) Berendsen, H. J. C.; Postma, J. P. M.; van Gunsteren, W. F.; DiNola, A.; Haak, J. R. Molecular Dynamics with Coupling to an External Bath. *J. Chem. Phys.* **1984**, *81*, 3684−3690.
(74) Sokal, R.; Michener, C. A Statistical Method for Evaluating Systematic Relationships. *Univ. Kans. Sci. Bull.* **1958**, *38*, 1409−1438.
(75) R Development Core Team R: *A Language and Environment for Statistical Computing*; Vienna, Austria : the R Foundation for Statistical Computing, 2014. ISBN 3-900051-07-0. Available online at http://www.R-project.org/.
(76) Soetaert, K. *plot3D: Plotting Multi-Dimensional Data*, R package version, 2013, https://cran.r-project.org/package=plot3D.
(77) Johnson, P. *Graphics Output Device*, 2015, https://cran.R-project.org/package=devEMF.
(78) Lemon, J. *Plotrix: A Package in the Red Light District of R*, R-News, 2006; Vol. *6*, pp 8−12.

DOI: 10.1021/acsomega.8b00128
ACS Omega 2018, 3, 2865−2882